Complementary transcriptome and proteome analyses provide insight into floral transition in Bamboo (Dendrocalamus latiflorus Munro)

Xiaoyan Wang
Kunming Institute of Botany Chinese Academy of Sciences
Yujiao Wang
Kunming Institute of Botany Chinese Academy of Sciences
Guoqian Yang
Shanghai Jiao Tong University
Lei Zhao
Kunming Institute of Botany Chinese Academy of Sciences
Dezhu Li
Kunming Institute of Botany Chinese Academy of Sciences
Zhenhua Guo (guozhenhua@mail.kib.ac.cn)
Kunming Institute of Botany Chinese Academy of Sciences

Research article

Keywords: floral transition, iTRAQ, biomarker gene, mRNA-protein correlation, bamboo

Posted Date: February 13th, 2020

DOI: https://doi.org/10.21203/rs.2.23428/v1

Complementary transcriptome and proteome analyses provide insight into floral transition in Bamboo (*Dendrocalamus latiflorus* Munro)

Xiaoyan Wang [1, †], Yujiao Wang[1, 2, †], Guoqian Yang [1, 3], Lei Zhao [1], Dezhu Li[1, *], Zhenhua Guo[1, *]

* Correspondence: dzl@mail.kib.ac.cn; guozhenhua@mail.kib.ac.cn

[1] China Southwest Germplasm Bank of Wild Species, the Key Laboratory of Biodiversity and Biogeography, Kunming Institute of Botany, Chinese Academy of Sciences, Kunming 650201, China;

Full list of author information is available at the end of the article

[†] Equal contributors: Xiaoyan Wang and Yujiao Wang contributed equally to this work.

Email addresses:

Xiaoyan Wang, cc11wxy@126.com

Yujiao Wang, wangyujiao@mail.kib.ac.cn

Guoqian Yang, guoqian.yang@sjtu.edu.cn

Lei Zhao, zhaolei@mail.kib.ac.cn

Abstract

Background

Most woody bamboos flower only once after long vegetable growth phases and die immediately afterward. It is difficult to know the timing of the floral transition, as little information is available on the molecular mechanism of plant maturity in bamboos.

Results

In this study, through RNA sequencing of leaves of D. latiflorus during floral transition and *de novo* assembly, a final set of 155,494 unigenes were obtained with N50 of 2,069 bp. We identified a lot of flowering time-associated and flowering integration genes and the continued increase and decrease genes were screened as flowering biomarker genes, such as *MADS14*, *bHLH13*, *ABA-related* genes. The different genes were assigned to specific metabolic pathways by Kyoto Encyclopedia of Genes and Genomes (KEGG) and the photoperiod pathways depending on the circadian rhythm may play an essential role in the bamboo floral transition. In addition, a total of 721 different expressed proteins of leaves from the vegetable-to-reproductive stages in the same flowering clumps were identified using iTRAQ technique. The correlations between the expression levels of a transcript and the abundance of its corresponding protein were observed infrequently, but the very strong correlation in the specific metabolic process was observed, such as carbon metabolism, sugar metabolism, and photosynthesis, underlining the importance of these metabolic pathways during floral transition.

Conclusions

In this report, we combined transcriptome with large-scale quantitative proteomes to investigate the flower transition of *D. latiflorus*. This work will provide insights into mechanism of floral transition for bamboos, and management of forest breeding.

Keywords: floral transition, iTRAQ, biomarker gene, mRNA-protein correlation, bamboo

Background

All organisms go through a series of distinct developmental phases during their growth (1) The transition to flowering is a critical step in the developmental phases. The genetic and biochemical routes by which sensing such cues influences flowering are often referred to as flowering pathways: vernalization and autonomous pathways, photoperiod pathway and the circadian clock; gibberellin pathway; ambient temperature pathway; age pathway and meristem responses (2-4). Multiple floral stimulus eventually moves from the leaves to the shoot apical meristem (SAM), a group of stem cells in the shoot apex, where they are converted to local cues that evoke the developmental phase transition (5, 6).

Bamboos can be classified into three categories based on flowering behavior: species which flower annually, species which flower gregariously and periodically, and species which flower irregularly (7). Most woody bamboos belong to the second category, and semelparity that flower once and die (8, 9) at the end of 3-120 years or more long vegetative growth phases (10). Many bamboos have a special life history trait of monocarpic mass flowering and death, suggesting a special genetic mechanism controlling floral transition in bamboos. This collective death of bamboos results in considerable loss to forest agencies and private cultivators, and also produced serious ecological crises, most strikingly for the giant pandas (11-13). Systematical theories on bamboo flowering mechanism has not yet been achieved,

and the studies done mostly focus on discussing the behaviors of flowering and analysis of genes role in flowering (14-16). With the development of high-throughout sequencing technology, a lot of genes of bamboo flowering had been identified (17-20). But to date, studies have been done primarily on flower development but little on the floral transition in bamboos has been investigated.

In model plants and other nonmodel plant species with large and non-sequenced genomes, transcriptome and proteome profiling are powerful methods to analyze dynamic changes in multiple biological processes, *e.g.* during development or external environmental stimulus (21). Transcriptomic and proteomic analyses are extremely efficient methods for identifying differential expression genes at the whole-genome level. The recently developed isobaric tags for relative and absolute quantitation (iTRAQ) technology was proven to be very efficient in protein profiling (22-24). However, because of the length of bamboo special flowering mechanism phase, it is difficult to get the material. In the present study, we found the *D. latiflorus* as an ideal bamboo. *D. latiflorus* (Bambusease, Bambusoideae, Poaceae), belonging to woody bamboo, is the most widely distributed and cultivated grass in southern China (25)**.** The biological characteristics of flowering and the regeneration process of *D. latiflorus* were investigated from 2008 to 2012. The clump of *D. latiflorus* flowered when mother culms died, followed by the surviving rhizome system, a few culms continued to flower each July to October during the next 3 years. Compared to the previous study, this is the first time to collect the serial sampling in the bamboo floral transition. We sequenced the samples by RNA-seq in the different bamboo culms. To determine the mechanism of floral transition of bamboos in the same flowering culms, we cataloged differences in the abundance

of mRNAs and proteins by integrated profiling of gene activity using RNA-seq and iTRAQ. Comparisons of transcriptome and proteome data provided novel indications as to which processes matched to floral transition are regulated at the level of the transcriptome and which are controlled at the proteome level. The transcriptome and proteome profiling will provide a supplement for the *D. latiflorus* genome resource. The study aims are to identify a set of candidate genes and pathways associated with the floral transition in bamboo. Our findings are expected to outline the mechanism of flowering, overcoming a barrier for conventional bamboo propagation technology.

Results

Leaf microstructure and chlorophyll fluorescence of *D. latiflorus*

We collected leaves from four stages, including leaf of vegetative clumps(L0), leaf from flowering clumps, and the second stage can be broken into 3 periods: leaf from non-flowering clumps (L1), big and small leaf from flowering clumps (L2, L3). The surface area of blade and the stomata in the middle cross-sectional blade were calculated and studied (Figure 2A-a). The leaf area significantly decreased from L0 to L3 ($P<0.01$, L0>L1>L2>l3, Figure 2A-b). The transection of the leaf blade is shown in the Figure 2A-c. They are the same structure without Kranz anatomy in the four stages. In the Figure 2A-d, the blade thickness of L0 is significantly thicker than of L1, L2 and L3 ($p<0.01$). The epicuticle thickness of L1 is significantly thicker than of L0, L 2 and L3 ($p<0.01$). The thickness of blade, epidermis and epicuticle has no differences in the L2 and L3 ($p>0.05$). The comparative morphology of leaf stomata by SEM was displayed in Figure 2A-e. It showed the mean stomatal length in the vegetative clumps (L0) was significantly longer ($P <0.01$) than of L1, L2 and L3 in the

flowering clumps. However, there were no significant differences ($p > 0.05$) between L2 and L3 (Figure 2A-f). The stomata density per square centimeter of leaf surface in the vegetative clumps (L0) is almost the same as that in the flowering clumps (L1, L2 and L3). In the present study, the parameters of chlorophyll fluorescence (Fv/Fm, Y[II], NPQ and qP) had significantly differences between the L0 and L3 ($P<0.01$) (Figure 2B-a). The curves of ETR from L0 to L3 were changed with light intensity (Figure 2B-b). It showed the linear relationship between electron transfer reactions (ETR) and photosynthetic active radiation (PAR). ETR rapidly increased with the increase of light intensity and gradually saturated at 300 μ mol / (m2 • s). The electron transfer ability of L0 is the strongest in the same local environment. The L0 value of ETR was the highest, followed by L1, L2, and L3.

The measurements of parameters from L0 to L3 were clustered by heat map (Figure 2C). The hierarchically clustered heat map showed the relationship in the development of morpho-physiological characteristics of the leaves at different stages during floral transition. It showed that L0 and L1 have similar developmental characteristics and L2 and L3 have similar developmental characteristics.

Illumnia sequencing, *de novo* assembly and preparing the reference sequences

In the study, 12 cDNA libraries (four stages, with three biological repeats) were constructed from total RNA of L0, L1, L2 and L3 respectively, and pair end sequenced using the Illumina Hiseq^{TM}2000 platform. In total, 207.68 million paired-end reads were generated. After cleaning and quality checks, the reads were assembled 2069 into contigs by Trinity. A final set of 155,494 unigenes were obtained, and the average unigene size is 1,477 bp, and

N50 is 2,069 bp (Table 2). The size distributions of these unigenes are shown in Figure 3. The assembly produced a substantial large number of unigenes. 125,293 unigenes were more than 1000 bp in length (Figure 3). We mapped our RNA-seq reads back to the constructed reference sequences, and 80% of which mapped to the reference sequences (Table 1).

To investigate the extent of variability among the biological replicates, we calculated the coefficient of variation of FPKM values for each gene between the replicates. The box-plot distribution of the log FPKM values is shown in Additional file 1: Figure S2 and demonstrates the median and the quartile values among the samples being compared for differential expression are almost identical. More than 80% of the genes in the samples had a variation coefficient less than 20% (Additional file 1: Figure S3), indicating a strong match among the biological replicates.

Screen and functional annotation of the differentially expressed genes (DEGs)

In this study, differentially expressed genes in L0, L1, L2 and L3 were identified by RSEM and “edgeR” package. The DEGs in L0 vs L1, L0 vs L2, L0 vs L3 were identified as 3,179, 1,732 and 4,376, respectively (Figure 4A). To functionally categorize the DGEs, Gene Ontology (GO) terms were assigned to each transcript by the best BLASTx hit from the Nr (Non-redundant protein sequence) database. The annotated unigenes were further categorized into three main groups: biological process, cellular component and molecular function. A total of 1,861 and 2,478 sequences (58.5% and 56.6% of all the unigenes) were categorized into 44 functional groups in the L0 vs L1 and L0 vs L3. However, a total of 988 unigenes (57% of all

the unigenes) were categorized into 41 functional groups in the L0 vs L2. The function of extracellular region, metallochaperone and nutrient reservoir was not found in the L0 vs L2 (Figure 4B).

To predict and analyze the function of the DEGs, non-redundant sequences were submitted to a BLASTx (E-value $\leqslant$ 10-5) search through the following databases: NR database, UniprotKB database and KEGG. The summary listed in the Table 3. For the L0 vs L1, L0 vs L2 and L0 vs L3, we found that a total of 3,045, 1,670, and 4,128 (95.8%, 96.4% and 94.4% of all unigenes, respectively) unigenes provide significant BLAST results in NR based on sequence homologies. A BLAST analysis of the assembled unigenes against the KEGG database showed that 1,289, 709 and 1,719 unigenes, were annotated with corresponding Enzyme Commission (EC) numbers and assigned to the reference canonical KEGG pathways.

To further test the reliability of the results from the next generation sequencing platform, qRT-PCR analysis was performed for 18 of the differentially expressed transcripts. The 18 genes transcripts were manually selected as representatives primarily focused on the function of floral transition, photosynthesis, stress-relative (Additional file 2: Table S1). The expression patterns of 17 genes detected by qRT-PCR fit well with those from RNA-seq results, except unigene 33763 annotated as a putative UVB-resistance protein (Additional file 1: Figure S4).

Screen candidate marker genes

Leaves from L1 to L3 were in the culms of the same bamboo flowering clump (sympodial). The gene expression profiles were illustrated and showed 618 genes were the

common DEGs during floral transition in Figure 5A. The 618 candidate genes were shown by a cluster analysis based on the k-means method (46). Five expression patterns (clusters) of the 618 DEGs were identified (Figure 5B). Cluster 1 is the most abundant group, which contained 247 genes that down-regulated at L2 and then up-regulated at L3. The clusters 2 and 5 consist of 152 and 65 genes, respectively, whose expression showed up-regulated at L2 and then down-regulated at L3. A difference in the gene expression levels of cluster 5 at L3 was lower than of cluster 2 at L1. The cluster 3 was composed of 82 genes which showed a continuous down-regulation during floral transition. Cluster 4 contained 72 genes which revealed a continuous up-regulation from vegetable growth to reproductive growth.

Hierarchical cluster sample analysis gives an overview of the total 618 unigenes (Figure 5C). We focused on the continued decrease (82 genes) and increase (72 genes) of the genes during floral transition (from L1 to L3). Of these, we choose the 18 genes by the annotations (Blastx and GO) which have significant biological functions as potential biomarkers (Additional file 2: Table S2). The function of some genes (unigene 138210, unigene 43312 and unigene 29008) is focused on loosening an extension of plant cell walls by disrupting non-covalent bonding between cellulose microfibrils. Genes specifically involved in regulating floral architecture and plant development (unigene 10723 and unigene 114865) displayed the up-regulation. The unigene 39652 coded MADS 15 protein transcript level was extremely low in vegetable leaves L1. Compared to vegetable leaves (L1), the expression of the chloroplastic protein (Unigene 41907: Far1-related sequence 5; Unigene 13665: Serine/threonine-protein kinase STN8, chloroplastic; Unigene 14850: Transcription factor bHLH13) was down-regulated in flowering leaves (L2 and L3). It is consistent with the

results of the photosynthetic rate decrease by the chlorophyll fluorescence (Figure 2B). In addition, the expression level of unigene 99180 which is involved in the regulation of stomatal aperture showed continued decrease from L1 to L3, which is consistent with the results in Figure 2A-e. The expression levels of stress-related genes, such as unigene 38555, promote plant stress tolerance such as heat, chilling, salinity and toxicity; unigene 72242-inactive ADP-ribosyltransferase that functions with SRO1 to regulate oxidative stress, hormonal and developmental responses; unigene 27191 may be involved in oxidative stress response, displayed a decline during the floral transition. In addition, the levels in the genes modulating plant transpiration efficiency by controlling stomatal density (unigene 133805, unigene 99180) decreased during bamboo flowering. The genes levels specifically involved in sugar transport protein (uniegene 21870) displayed the obvious down-regulation.

Identifying *D. latiflorus* flowering time-associated genes and senescence-associated genes

We screened the flowering time-associated genes which were assigned into different pathways (47) (Additional file 1: Figure S5). They consist of Autonomous pathway, vernalization pathway, photoperiod pathway, gibberellin pathway and aging pathway. The main genes associated with flowering time are displayed in Table 4. These included floral integrator pathway genes such as *FT*, *SOC1* and *AGL24*; vernalization pathway genes related to *Frigida (Fri)* and *VIN3*; autonomous pathway genes *FCA* and *FY*; gibberellin pathway genes *GID1*; floral meristem identity gene *AP1/FUL-like* genes *MADS14*; aging pathway gene *SPL9* and other flowering-related genes *AGL6* and *EMF1*; all these were identified in our *D. latiflorus* RNA-seq database. Most of these genes showed down-regulation at L3

compared to that at L0. Some senescence-associated genes were dominantly expressed in reproductive tissue L3. Of them, the FPKM value of Unigene 25575 demonstrated higher expression levels than other genes, the highest in L3 of the four stages (Figure 6B).

Pathways involved during floral transition in D. latiflorus and mobile signals controlling photoperiod-dependent flowering

We focused on the DEGs in the L0 vs L3. In total, 1,719 sequences (39.3% of all the unigenes) were assigned to 285 KEGG pathways. The pathways with most representation by the unigenes were metabolic pathways, genetic information processing and signaling and cellular processes. These pathways provide a valuable resource for investigating specific processes, functions and metabolic pathways during floral transition in *D. latiflorus*. We found 55 unigenes involved in plant hormone signal transduction, which contained 8 pathways (Additional file 1: Figure S6, Additional file2: Table S3). The hormone included auxin, cytokinin, gibberellin, abscisic acid, ethylene, brassinosteroid and jasmonic acid. In the study, the photoperiod pathway depending on the circadian rhythm was inferred. Several circadian clock-controlled genes (16 unigenes, 0.93%) regulating photoperiodic flowering in *D. latiflorus* were found in the pathway.

In the metabolic pathway dependent on the circadian rhythm regulating flowering (Figure 7A), some key genes (Table 5) observed to be up-regulated in L3, such as Two-component response regulator-like *APRR5* (*PRR5*), which exhibited 10 times higher expression than in L0. The actual expression level of *CO* and *FT* were performed (Figure 7B); the *CO* gene expression was up-regulated at YL1 compared to YL0, then down-regulated from YL1 to YL4. It showed a higher expression level at L3 than that at L0 in the adult phase.

The FT gene expression was down-regulated from YL0 to YL4 and up-regulated at L0, then displayed continued rising from L1 to L3, the expression level at L3 lower than that at L0.

To determine the *COL* gene family of *D. latiflorus*, we analyzed the gene functions and found 15 unigenes were annotated as zinc finger protein CONSTANS (Additional file 2: Table S4). We selected 7 unigenes with two conserved B-box domains and a CCT domain to further examine their relationship with other *COL* genes in Poaceae (such as *Zea mays*, *Setaria italic*, *Hordeum vulgare* and *Brachypodium distachyon*). The amino acid sequences of 7 unigenes were used to construct a phylogenetic tree. As shown in Additional file 1: Figure S7, these unigene sequences showed a very high similarity (100% identity) to genes isolated from other gramineous plant species.

In the present study, in addition to the FT as a florigen, which is a mobile signal, we have found others controlling photoperiod-dependent flowering, such as Auxin, Gibberellin, Cytokinin, Abscisic adid, Salicylic acid, Ethylene and Brassinosteroid, and sugar (Additional file 2: Table S5).

Proteomics analysis

A total of 4,636 proteins were identified and listed in Additional file 3. Out of 4,636 hits in the public databases, 4,282 protein sequences were classified into 24 COG categories (Figure 8), among the 24 “General function prediction only” represents the largest group (729; 17.02%), followed by “Carbohydrate transport and metabolism” (455; 10.63%), “Posttranslational modification, protein turnover, chaperones” (418; 9.76%) , “Energy production and conversion” (363; 8.48%) and “Translation, ribosomal structure and biogenesis” (359; 8.38%). “Cell motility” (2; 0.05%) and “Nuclear structure” (2; 0.05%) were

the smallest groups. To obtain functional information about these identified proteins, Blast2GO was searched for biological processes, cellular proteins and molecular functions. We found 57 proteins in total related to flowering (Additional file 4), such as regulation of flower development protein, flowering-promoting factor 1-like protein 3, and negative regulation of flower development protein.

A 95% confidence level ($P < 0.05$) and a 1.2-fold change were used to identify proteins that were differentially expressed between L1 and L2 during floral transition (Figure 9). Using these criteria, 721 differentially expressed proteins (282 up-regulated in Additional file 5 and 439 down-regulated in Additional file 6) were found. The 721 differentially expressed proteins were searched against the KEGG pathway with 397 proteins significantly enriched ($P<0.05$) in 8 metabolic pathways (Table 6). Notably, 44 differential proteins were predicted to be involved in photosynthesis-related pathways (Photosynthesis: 29; 5.1%; Photosynthesis-antenna proteins: 15; 2.64%) during floral transition. Many proteins were mainly focused on the “Metabolic pathway”, “Ribosome”, “Phenylalanine metabolism”, “Peroxisome”, “Sulfur metabolism”, “Valine, leucine and isoleucine biosynthesis”.

Integrative analysis of the proteome and transcriptome of L1 and L2

There were 65 identified proteins that had corresponding transcripts in the RNA-seq data (Additional file 7). The P977 as a vegetative storage protein had a high relative with the corresponding transcript. Most focused on the chloroplastic-like proteins, others belong to unknown or hypothetical proteins.

The distribution of the corresponding mRNA: protein ratio is shown by a scatterplot analysis of the $\log_2$-transformed ratios (Figure 10). The Pearson correlation coefficients for

these data is 0.48 ($P<0.05$). We used the 65 proteins and the corresponding transcripts in our transcriptome databases, which had high correlation between the proteins and corresponding transcripts, to search through the KEGG databases. The pathways were mainly focused on biosynthesis of secondary metabolites, carbon metabolism, starch and sucrose metabolism, photosynthesis and spliceosome (Table 7). Of all of these, the highest correlation between protein and mRNA abundance in L1 and L2 were focused on the carbon metabolism, Photosynthesis, and starch and sucrose metabolism.

Discussion

Bamboo flowering is a highly coordinated, genetically programmed process with the change of leaf size as a particular phenomenon. Little is known about the mechanisms responsible for floral transition and genomic information for *D. latiflorus*. According to morphological leaf form during floral transition in *D. latiflorus*, the developmental processes were divided into four stages (L0, L1, L2 and L3), and RNA-seq uncovers the four development stages of leaf transcriptome landscape. The availability transcriptome data for *D. latiflorus* would meet the initial information needs for functional studies of this species and its relatives. With technological advances, in particular in mass spectrometry and high-throughput cell imaging, have allowed for large-scale surveys of the proteome (48). The study of leaf anatomical structure and chlorophyll fluorescence in the *D. latiflorus* (Figure 2C) demonstrated these characteristics in L1 are different from that in L2. Floral transition from L1 to L2 is a critical point. We selected the L1 and L2 in the same flowering clumps with the same biological background to study proteomics characterization by iTRAQ during floral transition; a supplement for the description of the transcriptome. Both the transcriptomic and

proteomic data are important in deciphering the molecular processes involved in floral transition.

Identifying genes associated with *D. latiflorus* flowering time

Of all the identified genes, genes regulating flowering time in the most important pathway are shown in Table 4. Of these pathways, encoding the genes *FRI* (*Frigida*, unigene 57034), *FLC* (*Flowering locus C*, unigene49361), *VIN3* (*Vernalization-insensitive 3*, Unigene110221) are known to be vernalization. *FRI* is a floral repressor and plays a key role in the Arabidopsis flowering time. Dominant alleles of *FRI* confer late flowering, which is reversed to earliness by vernalization. Loss-of-function mutation at *FRI* has provided the basis for the evolution of many early-flowering ecotypes (49). In this study, we found the gene *FRI* expression level is higher in L0 (Vegetable state) than L3 (reproductive state). This finding is in agreement with previous results from *Phyllostachys violascens* showing that *PvFR*I was expressed in all tested organs with a higher expression in non-flowering than in flowering plants (50). In response to vernalization, the *FLC* mRNA and protein is reduced (51), and therefore vernalization promotes flowering by the reduction of *FLC* expression. Our material was not exposed to cold temperature. The *FLC* gene expression level in L3 is higher than L0 in natural environments.

In this study, the genes associated with gibberellin pathways included the genes *GID1* (Unigene132606), *GA20ox* (Unigene33012). Gibberellins (GAs) consist of a large group of tetracyclic diterpenes, a few of which are endogenous growth regulators and play roles in plant growth and development (52). GA receptor (GID1) is a key mediator of GA response pathways. By binding to a nuclear receptor, GID1, gibberellins regulate gene expression by

promoting degradation of the transcriptional regulator DELLA proteins, including GIBBERELLIN INSENSITIVE (GAI) (53). Mutant and expression analyses demonstrated enzymes catalyzing the early steps in the GA biosynthetic pathway are mainly encoded by single genes, while those for later steps (i.e. *GA20ox*) are encoded by gene families (52).

We also identified the genes *FCA* and *FY*, belonging to autonomous pathway; *FCA* and *FY* are involved in one sub-pathway, and interact to regulate RNA processing of *FLC* in *Arabidopsis* autonomous pathway. In addition, Sequence homologs for *AGL6* and *EMF1* are found in our database. *AGL6* genes are MADS-box genes expressed in floral tissues which regulate floral organ identity and floral meristem determinacy (54). *EMF1* is involved in delaying both the vegetative to reproductive transition and flower initiation in Arabidopsis (55). Vegetative phase change is initiated by a decrease in the expression of miR156 and consequent increase in the expression of SBP genes i.e. the paralogous genes *SPL9* in newly formed organs (56). The *SPL* gene expression in L0 is higher than in L3 in the present study. Consistent with the finding, we discovered the size in L0 is significantly larger than in L3 by the quantitative statistics of bamboo leaf size (Figure 2A).

Identification of flowering integration genes and metabolism pathways involved in floral transition

In this study, three integration genes, including *SOC1*, *AGL24*, *FT*, all of which are at the point of convergence of several flowering-time pathways, have been identified. The gene structure of *SOC1* is significantly different between woody and herbaceous bamboos, which is potentially the cause of long vegetative stage in life of woody bamboos (17). *AGL24* plays a role in the regulation of flowering time, which is a promoter of flowering and acts as a

positive regulator of *SOC1* (57). In bamboo, recently research found *PvFT1*, which is a candidate gene for florigen, the expression of *PvFT1* reached its highest level 20 to 30 days before flowering in the leaves (58). In the present study, compared with L0, the expression level of *FT* genes showed a decline in L3 (Table 5). We can conclude that the FT protein moves into the SAM during floral transition in *D. latiflorus*. Future study of floral transition in bamboo may find this is a crucial candidate gene.

A number of genetic pathways controlling flowering time have been identified in Additional file 1: Figure S5. We focused on the photoperiod pathway that depends on the circadian clock (Figure 7). The photoperiod pathway controls this response in the leaves through a signaling cascade involving *GIGANTEA (GI)* and the transcriptional regulator *CONSTANS (CO)* and FT gene (59). Light signals are first received by two photoreceptors, phytochromes (PhyA, PhyB, PhyC, PhyD, PhyE) and cryptochromes (Cry1, Cry2) (60-62), which process the physical signals and produce a circadian rhythm (63-65). *TIMING OF CHLOROPHYLL A/B BINDING PROTEIN*1 (*TOC1*), *LATE ELONGATED HYPOCOTYL* (*LHY*) and *CIRCADIAN CLOCK ASSOCIATED1* (*CCA1*) are the parts of the central mechanism generating circadian rhythms in plants (66). *LHY* and *CCA1* were proposed to act along with *TOC1* in transcriptional-translational negative feedback loop (67, 68). The photoperiodic genes also play an important role in bamboo flowering (69). This study elucidates the photoperiodic regulation of bamboo homologs of important flowering genes. In this study, sequences homologues for genes involved in regulation of the circadian clock described above (*Phy*, *GI*, *EIF*, *APRR*, *LHY*, *CCA1*, *COP1*) were listed in the table 5. The main DEGs in the L3 depending on the circadian rhythms regulating flowering during floral

transition were up-regulated compared to that in the L0.

The long juvenile phase of bamboo is not obviously regulated by day length. To determine whether the bamboo *CO*/*FT* ortholog is also involved in the regulation of flowering time, we analyzed the *CO*/*FT* gene expressions as the core of the pathway that promotes flowering (Figure 7A). We collected leaves from bamboo seedlings aged 3 months to 6 years. Figure 7A-B showed decrease during the juvenile phase of bamboo. The expression levels from YL0 to YL3 and L0 to L1 display decrease, and may have genes acting as repressors of *FT* transcription, or leaf-derived signals such as *FT* are transported to particular meristems, not the meristems that can be induced to form flowers (8). When adult bamboo was in the vegetable state (L0, adult vegetable state), the expression showed a high level compare to juvenile stages. Compared with a previous study that the highest expression level of *FT* homologs were detected in the flowering clumps in bamboo species (*Phyllostachys meyeri and Shibataea chinensis*) (70), it is consistent with our results which displayed a higher expression in the L3 (reproductive state) than in the L1 (vegetable state) of the same flowering clumps. The *FT* transcript expression displayed a gradual increase as bamboo grew older from L1 to L3, suggesting that a critical level of *FT* expression is needed to initiate flowering.

In contrast to *FT*, *CO* mRNA cycles regardless of day length, with a prominent peak in the night following either a long or short day, and an earlier shoulder in afternoon only in long days (71, 72). CO protein promotes the transition from vegetable growth to flowering (73). The gene *CO* expression level decreased from YL1 to YL4 during juvenile stages. This may be why bamboo will wait so long to flower. For the same flowering clump, it revealed the

highest expression level in L1, and then after that bloomed. Contrary to the FT gene which showed the lowest expression level in L1, we speculated it was produced by the mobility of FT protein-this needs further experimentation. 15 unigenes containing the conserved CCT domains were identified (Table 6). Nine genes were used to perform the phylogenetic analysis (Figure 7). The sequence data showed a high similarity with these genes in other homologous species (*Zea mays*, *Setaria italic*, *Hordeum vulgare* and *Brachypodium distachyon*). They are the regions with higher homology represent units of functional importance.

In the case of floral induction by photoperiod, long-distance signalling is known to occur between the leaves and the SAM via the phloem (74), such as hormones (Auxin, Abscisic acid, Cytokinin, Abscisic adid, Salicylic acid, Ethylene and Brassinosteroid) and sugar (Additional file 2: Table S5). These appeared to function as other key signals in the regulation of bamboo flowering. They are important resources for the study of floral transition and flower organ development in the future. More studies on their expression patterns and their functions in the future will help to outline the floral mechanism.

Screened floral biomarker genes

To better understand the information related to gene expression of *D. latiflorus*, we analyzed the gene expression patterns under different developmental phases. Our analysis identified 618 genes commonly differentially expressed in L1 vs L2 and L2 vs L3, and potentially affecting the floral transition in *D. latiflorus* (Figure 5). We found the gene expression profiles in the compared samples. 5 groups were defined according to their expression profiles. We focused on the genes, which showed continuous up-regulated and down-regulated, and can be screened for the candidate genes predicting the identity of the

bamboo clump that gave rise to vegetative or reproductive state. In Figure 2B-a, the Fv/Fm ratio of L3 is significantly lower than of L1, and showed the reproductive bamboo was inefficient, with low nutrient and low photosynthesis (75, 76). These results were consistent with the RNA-seq, i.e. the gene controlled photosynthesis and stress-resistance, whose expression level continued to decrease from L1 to L3 (Additional file 2: Table S2). The bHLH13 transcription factors function redundantly to negatively regulate Jasmonates-mediated plant defense and development (77). Jasmonates (JAs) regulate diverse aspects of plant developmental processes, such as senescence (78, 79). In the present study, the transcription factor *bHLH13* decreased during floral transition. The Jasmonates-related genes may increase from L1 to L3, and then will increase the expression of leaf senescence-associated genes. The *MADS14* is induced in the SAM during meristem phase transition (6). In our study, the *MADS14* gene expression level increased during floral transition. It would play an important role in phase transition in bamboo. We found the progression of bamboo flowering is accompanied by the rapid loss of chlorophyll, the decreased abundance of photosynthesis-related proteins, and the increased expression of senescence-associated genes, *ABA* and *MADS14*. This may be the reason for masse death of bamboo after flowering. This study suggests that losing the soil, killing the grass, and fertilizing would help to develop sustainable management of *D. latiflorus*.

Protein changes and metabolism relate to floral transition

Our iTRAQ data obtained from the L1 (vegetable state) and L2 (reproductive state) proteins provided a genome-scale proteomic analysis of bamboo floral transition. According to the COG annotation of 4,282 protein sequences, we concluded that “Carbohydrate

transport and metabolism" plays a central role on the floral transition of *D. latiflorus* (Figure 8). In our transcriptome data, we identified the SUS (sucrose synthase) and Tre6p (Trehalose-6-phosphate) (Additional file 2: Table S5). Corbesier et. al. showed an increased export of carbohydrates by leaves and starch mobilization are critical for induce flowering in *A. thaliana* (80).

Here, comparison of the L1 (vegetable state) and L2 (reproductive state) leaves proteomes in *D. latiflorus* revealed 721 proteins differentially expressed during floral transition (Figure 9), which account for 15.55% of the proteins we identified. Of the 721 proteins, 65 corresponded to the unigenes that were obtained by RNA-seq. In the present study, 78.5% (55 out of 65) of the protein and transcript pairs decreased or increased in parallel during floral transition. Of the 51 proteins, 7 have significantly decreased and only 1 protein have significantly increased (Additional file 7). This proteomic change is the same order of magnitude as the genes at transcriptional level, such as the carbon metabolism, photosynthesis, and starch and sucrose metabolism pathway. However, a direct comparison of protein and their corresponding mRNA expression levels revealed poor correlations (r=0.48) and few overlapped significant changes (Figure 10). This finding is in agreement with previous studies about various organisms showing a large number of genes exhibited inconsistency between the transcript protein levels, which Pearson correlation coefficients for these data range from 0.46 to 0.76 (81-83) and a substantial regulatory process occurring after mRNA is produced (post-transcriptional, translational and protein degradation regulation) (48). In our proteomic sequence, we found the function of 418 identified proteins, which account for 9.02% of the proteins we identified, focused on posttranslational modification,

protein turnover, and chaperones, and it showed that major genes related to flowering produce proteins that exist in posttranslational modification in bamboo. Post-transcriptional and translational processing regulates the location, quantity, and efficiency of the proteins in the cell. The relationship between mRNA and protein abundances is complex due to the series of regulatory processes. Schwanhausser et al. showed that mRNA was produced at a much slower rate than the rate of protein translation and protein products were five times more stable and 2800 times more abundant than mRNAs in mammalian cells (84). Therefore, expression changes detected at the mRNA level may or may not result in variable protein abundance. In our study, we found P977 (vegetative storage protein PNI288) has a high consistency with the corresponding transcript. PNI288, which is one subfamily of bark storage proteins (BSP) family, plays overlapping but non-redundant roles in N storage (85). Key processes of this N redistribution are autumnal leaf senescence and storage of released N as BSP in perennial tissues (86).

A striking feature of our proteomic data was that 57 proteins (Additional file 4) were identified as flowering-related proteins. The relative change in abundance (L2/L1) is shown with a $\log_2$ value between vegetable and flowering leaves in *D. latiflorus,* which were shown in Additional file 2: Table S3. *FPF1 (FLOWERING PROMOTING FACTOR 1)* is one important gene involved in the genetic control of flowering time in *Arabidopsis* (87, 88). In our present study, the FPF1 protein was identified. The candidate proteins would be selected for the functional study for *D. latiflorus* during floral transition. The stress resistance protein (Protein ID: P536, P1156, P768 and P639) and photosynthesis related protein (Protein ID: P3937) correspond to the transcript showed decrease in parallel during floral transition.

Therefore, the decreased function on stress and photosynthesis deserves further investigation as a potentially significant regulator for death after bamboo massive flowering, which is in accordance with the RNA-seq results. We have been shown bamboo flowering is the result of an orderly alteration of a series of physiological and biochemical events, such as ABA, sugar and acid metabolism, and each of these metabolic systems or processes is involved in the regulation of a number of genes. In our present study, we proposed a pathway model depending on the circadian rhythm to induce flowering in bamboo (Figure 11). This model involves metabolites, hormones and gene products interacting as long- or short-distance signalling molecules, which will lay the foundation for uncovering bamboo flowering.

Conclusions

In this study, we present the application of RNA-seq to leaves and report a comprehensive analysis of the transcriptome which will serve as a blueprint of the gene expression profile during floral transition. A multiple-level analysis of the gene/protein expression changes in L2, compared with L1, was conducted. These results revealed several key candidate regulators which may play important roles in bamboo floral transition. Combined with transcriptomic and proteomic data, we identified biological processes related to bamboo flowering, such as carbon metabolism and starch and sucrose metabolism. Thus, the integrated analysis enabled a comprehensive understanding of biological events relevant to the regulation of bamboo floral transition. Multiple flowering-associated events were shown to happen during floral transition; our data will provide new insights into the molecular mechanism of bamboo flowering regulatory network.

Methods

Sample preparation

D. latiflorus leaves were collected from each of the three flowering clumps and three vegetable clumps on 2011 near Longsuo village, Pengpu town, Mile county of Yunnan Province in southwest China (N24°02′13″, E103°22′26″). As *D. latiflorus* is not endangered, collection of samples for scientific purposes is permitted by local legislation. The plants were identified by Dr. Zhenhua Guo. The voucher specimen is accessible at the Herbarium of Kunming Institute of Botany, Chinese Academy of Science. All collected leaves were classified into four phases by the developmental process (see Figure 1 for details). Three vegetable and reproductive clumps of similar size and similar developmental stages were selected. At the second to third leaf position from the branch's top (in September after leaves stop growing), the three whole fully extended leaves were harvested. We collected bamboo seeds to germinate and tested different ages of the bamboo seedlings (Additional file 1: Figure S1). Samples were immediately frozen in liquid nitrogen and stored at -80℃ until RNA and/or protein was extracted, and other leaves stored in FAA (formalin: glacial acetic: 50% ethanol = 1:1:18) were used for morphology analysis.

Measurement of leaf surface area

Leaf area was measured using paper-cutting method described by Hattersley (26) with some modifications. Fresh leaves were collected and immediately processed for leaf area measurement. One A3 size paper was taken and its weight and area were measured. The leaf was then placed on the paper and its outline was drawn carefully. The paper within the outlined area was cut and weighed. The leaf area in cm^2 was calculated according to the following formula:

Leaf area=$\frac{a \times y}{x}$

where a=area of the A3 paper in cm^2, y=weight of the cut paper in g, x=weight of the A3 paper in g (27).

Leaf anatomy, leaf stomatal size and density measurement

For microscopic studies, leaf materials (4 × 4 mm) were cut next to the major first order vein at 50% of the whole leaf length. For the studies of paraffin sectioning, samples were fixed in FAA and dehydrated in a graded ethanol series. The samples were then embedded in Paraplast by LEICA EG 1160 (Leica Micosystems, Wetzlar, Germany). The paraplast was cut into 5 μm sections on a Leica RM2135 microtome and mounted on glass slides. The sections were then deparaffinized with xylene, stained with fast green, and analyzed using a Leica DFC 295 camera (Vashaw Scientific Inc, Wetzlar, Germany) attached to a Leica DM 1000. The rest were processed for SEM as previously described (28). The lower epidermis of leaves were coated in gold-palladium, and analyzed by a Hitachi S-4800 scanning electron microscope (Hitachi High-Technologies Corp., Tokyo, Japan). The leaf stomatal size and density were analyzed by software Image J (29).

Chlorophyll fluorescence detection in the *D. latiflorus*

The chlorophyll content of the four stages of leaves was determined using an Imaging-PAM chlorophyll fluorometer (Walz, Effeltrich, Germany). The leaves were in the dark room for 20 minutes. The instrument is driven by software that allows the user to control the timing, duration and intensity of each light source (LED measuring light panels, continuous blue actinic light and the blue saturating light pulses) (30).

Kinetic imagines of chlorophyll fluorescence depend on the continuous modulated light. To analyze the heterogeneity of chlorophyll fluorescence of leaves, at least 3 points were randomly picked on the surface of leaves. Each pixel vale among these three points and fluorescence parameters were automatically calculated (31) by Imaging Win software. All measured parameters were repeated at least three times.

RNA seq, data processing, and reference preparation

Total RNA of leaves in the four stages (L0, L1, L2 and L3) was isolated using RNAiso Plus (TaKaRa, Japan). Equal amounts of RNA collected from three independent experiments were used for sequencing respectively. RNA-seq libraries were constructed with methods as previously described (32). Finally, the pooled library was sequenced using Illumina HiSeq^{TM} 2000. High-quality reads (clean reads) were obtained by removing low-quality reads with ambiguous nucleotides, and adaptor sequences were filtered from the raw reads. De novo assemblies for these 12 datasets (leaves of the four stages of *D. latiflorus*, three biological repeats,) were performed separately by Trinity (release 20110713) (33). As there is not a reference genome available for *D. latiflorus*, the generated unigenes (hereafter referred to as dataset 1), the previously research in our group that retained transcriptome of floral buds (32) (referred to as dataset 2), root, leaf and seeds of *D. latiflorus* (34) (dataset 3) and the *D. latiflorus* EST data (release 20121230, referred to as dataset 4) were assembled into a reference by TGICL and were used to remove redundancy by CD-HIT-EST (35).

Screening of differentially expressed genes (DEGs)

RSEM (v1.1.11) (36) was used to quantify transcript abundance in each sample and then the RSEM-estimated fragment counts were fed into edgeR package (37). Gene expression bias was evaluated using Fisher's exact test of the edger package. According to the methods (25) of screening the key candidate genes that indicate the vegetable to reproductive phase change. Phase changed from L1 to L3 showed the floral transition in the same culms of flowering clumpling (sympodial). They were clustered using k-means, with k=100 and 1000 repeats of "k-means" function using the Gene cluster 3.0 (38) and Java Treeview software (39). The hierarchical tree was constructed using the function "gplots" from the R package "ggplot" (40).

To deduce the putative function, the differentially expressed genes were subjected to BLASTX analysis UniprotKB and NR database with a cut-off of 1E – 5. BLAST2GO program (41) was used to perform gene ontologies (GO) (42) annotation. We perform cluster analysis of gene expression patterns with cluster (38) software and Java Treeview (39) software.

Sequences were annotated by homology search against NCBI and aligned via Clustal W (43). The phylogenetic trees of homologous genes were constructed employing the neighbor-joining method of MEGA5.05 (44) with 1000 bootstrap replicates.

Quantitative real-time PCR (qRT-PCR) validation

Twenty pairs of primers were designed to generate amplicons for validating the RNA-seq data (Additional file 2: Table S2). Gene-specific primers designed using Primer Express 3.0. Aliquots of total RNA extracted for sequencing as described

earlier were used for quantitative real-time PCR (qRT-PCR) experiments according to the manufacturer's instructions (Roche, Shanghai, China). The *EF1α* gene (45)was used as a reference in all qRT-PCR experiments.

iTRAQ Labeling and SCX fractionation

Total protein (100μg) was taken out of each sample solution and then the protein was digested with Trypsin Gold (Promega, Madison, WI, USA) with the ratio of protein: trypsin = 30: 1 at 37°C for 16 hours. After trypsin digestion, peptides were dried by vacuum centrifugation. Peptides were reconstituted in 0.5M TEAB and processed according to the manufacture's protocol for 8-plex iTRAQ reagent (Applied Biosystems).

SCX chromatography was performed with a LC-20AB HPLC Pump system (Shimadzu, Kyoto, Japan). The iTRAQ-labeled peptide mixtures were reconstituted with 4 mL buffer A (25 mM NaH2PO4 in 25% ACN, pH 2.7) and loaded onto a 4.6×250 mm Ultremex SCX column containing 5-μm particles (Phenomenex). The peptides were eluted at a flow rate of 1mL/min with a gradient of buffer A for 10 min, 5-60% buffer B (25mM NaH2PO4, 1 M KCl in 25% ACN, pH 2.7) for 27 min, 60-100% buffer B for 1 min. The system was then maintained at 100% buffer B for 1 min before equilibrating with buffer A for 10 min prior to the next injection. Elution was monitored by measuring the absorbance at 214 nm, and fractions were collected every 1 min. The eluted peptides were pooled into 20 fractions, desalted with a Strata X C18 column (Phenomenex) and vacuum-dried.

LC-ESI-MS/MS analysis based on Q EXACTIVE

Each fraction was resuspended in buffer A (2% ACN, 0.1%FA) and centrifuged at 20000g for 10 min, the final concentration of peptide was about 0.5 μg/μl on average. 10μl supernatant was loaded on a LC-20AD nanoHPLC (Shimadzu, Kyoto, Japan) by the autosampler onto a 2cm C18 trap column. Then, the peptides were eluted onto a 10cm analytical C18 column (inner diameter 75 μm) packed in-house. The samples were loaded at 8 μL/min for 4min, then the 44min gradient was run at 300 nL/min starting from 2 to 35% B (98%ACN, 0.1%FA), followed by 2 min linear gradient to 80%, and maintenance at 80% B for 4 min, and finally return to 5% in 1 min.

The peptides were subjected to nanoelectrospray ionization followed by tandem mass spectrometry (MS/MS) in an Q EXACTIVE (Thermo Fisher Scientific, San Jose, CA) coupled online to the HPLC. Intact peptides were detected in the Orbitrap at a resolution of 70, 000. Peptides were selected for MS/MS using high-energy collision dissociation (HCD) operating mode with a normalized collision energy setting of 27.0; ion fragments were detected in the Orbitrap at a resolution of 17, 500. The electrospray voltage applied was 1.6 kV. Automatic gain control (AGC) was used to optimize the spectra generated by the orbitrap. The AGC target for full MS was 3e6 and 1e5 for MS2. For MS scans, the m/z scan range was 350 to 2000 Da. For MS2 scans, the m/z scan range was 100-1800.

Data Analysis and Functional Annotation

The MS spectra were analyzed by a thorough search using Mascot software (Matrix Science, London, UK; version 2.3.02) against NCBI_Poaceae (456,311

sequences). Search parameters were as followed: MS/MS ion search; trypsin enzyme; fragment mass tolerance 0.02 Da; monoisotopic mass values; variable modifications of Gln->pyro-Glu (N-term Q), Oxidation(M), Deamidated (NQ) as the potential variable modifications, and Carbamidomethyl (C), iTRAQ8plex (N-term), iTRAQ8plex (K). The charge states of peptides were set to +2 and +3. To reduce the probability of false peptide identification, only peptides with significance scores (≥20) at the 99% confidence interval by a Mascot probability analysis greater than "identity" were counted as identified. The quantitative protein ratios were weighted and normalized by the median ratio in Mascot. We only used ratios with p-values < 0.05, and only fold changes of >1.2 was considered as significant. Functional annotations of the proteins were conducted using Blast2GO program against the non-redundant protein database (NR; NCBI). The KEGG database (http://www.genome.jp/kegg/) and the COG database (http://www.ncbi.nlm.nih.gov/COG/) were used to classify and group these identified proteins.

Abbreviations

RNA-seq: high-throughput RNA sequencing; AP1: APETALA1; FUL: FRUITFULL; KEGG: Kyoto Encyclopedia of Genes and Genomes; SAM: shoot apical meristem; iTRAQ: isobaric tags for relative and absolute quantitation; ETR: electron transfer reactions; PAR: photosynthetic active radiation; GO: Gene Ontology; Nr: Non-redundant protein database; EC: corresponding Enzyme Commission; Fri: Frigida; PRR5:response regulator-like APRR5; GAs: Gibberellins; GAI: GIBBERELLIN INSENSITIVE; GI: GIGANTEA; CO: CONSTANS;TOC1: TIMING OF CHLOROPHYLL A/B BINDING PROTEIN1; LHY:

LATE ELONGATED HYPOCOTYL; CCA1: CIRCADIAN CLOCK ASSOCIATED1; SUS: sucrose synthase; Tre6p: Trehalose-6-phosphate; BSP: Bark Storage Proteins; FPF1 :FLOWERING PROMOTING FACTOR 1; DEGs: differentially expressed genes; HCD : high-energy collision dissociation; AGC: Automatic gain control.

Declarations

Ethics approval and consent to participate

Not applicable

Consent for publication

Not applicable

Availability of data and materials

The datasets used and analyzed during the current study are available from the corresponding author on reasonable request.

Competing interests

The authors declare that they have no competing interests.

Funding

This work is supported by grants from National Natural Science Foundation of China (31670227); the Strategic Priority Research Program of Chinese Academy of Sciences (XDB31000000). The funder made no significant role in study design, sample collection and data analysis, decision to publish, or writing of the manuscript.

Authors' Contributions

ZG and DL designed and supervised the study. Sampling were performed by XW and GY. XW completed most of the experiments. LZ analyzed data. XW and YW wrote the article. All author had read and approved the manuscript.

Acknowledgements

We give thanks to Yunnan university to provide technical support of the sequencing platform. We thank Professor Jinyong Hu give us guides for paper writing. We wish to thank all of the workmates in our lab to collect all the samples in the experiment.

Authors' information

[1] China Southwest Germplasm Bank of Wild Species, the Key Laboratory of Biodiversity and Biogeography, Kunming Institute of Botany, Chinese Academy of Sciences, Kunming 650201, China;

[2] University of Chinese Academy of Sciences, Beijing, China;

[3] School of Agriculture and Biology, Shanghai Jiao Tong University, Shanghai 200240, China

References

1. Poethig RS. Phase change and the regulation of shoot morphogenesis in plants. Science. 1990;250(4983):923-30.

2. Kim DH, Doyle MR, Sung S, Amasino RM. Vernalization: winter and the timing of flowering in plants. Annual review of cell and developmental biology. 2009;25:277-99.

3. Amasino R. Seasonal and developmental timing of flowering. Plant J. 2010;61(6):1001-13.

4. Cho LH, Yoon J, An G. The control of flowering time by environmental factors. Plant J. 2017;90(4):708-19.

5. Hempel FD, Welch DR, Feldman LJ. Floral induction and determination: where is flowering controlled? Trends Plant Sci. 2000;5(1):17-21.

6. Kobayashi K, Yasuno N, Sato Y, Yoda M, Yamazaki R, Kimizu M, et al. Inflorescence meristem identity in rice is specified by overlapping functions of three AP1/FUL-like MADS box genes and PAP2, a SEPALLATA MADS box gene. The Plant cell. 2012;24(5):1848-59.

7. Brandis D. Biological notes on Indian bamboos1899.

8. Bohlenius H, Huang T, Charbonnel-Campaa L, Brunner AM, Jansson S, Strauss SH, et al. CO/FT regulatory module controls timing of flowering and seasonal growth cessation in trees. Science. 2006;312(5776):1040-3.

9. Keeley JE, Bond WJ. Mast Flowering and Semelparity in Bamboos: The Bamboo Fire Cycle Hypothesis. Am Nat. 1999;154(3):383-91.

10. Janzen DH. Why Bamboos Wait So Long to Flower. Annual Review of Ecology and Systematics. 1976;7(1):347-91.

11. Chalavaraju BS, Singh MD, Rao MN, Ravikanth G, Ganeshaiah KN, & Shaanker RU. Conservation of bamboo genetic resources in Western Ghats: status, threats and strategies. Forest Genetic Resources: Status, Threats and Conservation Strategies. 2001:97-113.

12. John CK, Nadgauda RS. Review in vitro-induced flowering in bamboos. In Vitro Cellular & Developmental Biology-Plant. 1999;35(4):309-15.

13. Tian ZX, Liu XH, Fan ZY, Liu JG, Pimm SL, Liu LM, et al. The next widespread bamboo flowering poses a massive risk to the giant panda. Biological Conservation. 2019;234:180-7.

14. Liu J, Cheng Z, Xie L, Li X, Gao J. Multifaceted Role of PheDof12-1 in the Regulation of Flowering Time and Abiotic Stress Responses in Moso Bamboo (Phyllostachys edulis). Int J Mol Sci. 2019;20(2):424.

15. Ge W, Zhang Y, Cheng Z, Hou D, Li X, Gao J. Main regulatory pathways, key genes and micro RNA s involved in flower formation and development of moso bamboo (Phyllostachys edulis). Plant biotechnology journal. 2017;15(1):82-96.

16. Tian B, Chen Y, Li D, Yan Y. Cloning and characterization of a bamboo LEAFY HULL STERILE1 homologous gene. DNA Seq. 2006;17(2):143-51.

17. Guo ZH, Ma PF, Yang GQ, Hu JY, Liu YL, Xia EH, et al. Genome Sequences Provide Insights into the Reticulate Origin and Unique Traits of Woody Bamboos. Mol Plant. 2019;12(10):1353-65.

18. Yang Z, Chen L, Kohnen MV, Xiong B, Zhen X, Liao J, et al. Identification and Characterization of the PEBP Family Genes in Moso Bamboo (Phyllostachys heterocycla). Sci Rep. 2019;9(1):14998.

19. Cheng Z, Hou D, Liu J, Li X, Xie L, Ma Y, et al. Characterization of moso bamboo (Phyllostachys edulis) Dof transcription factors in floral development and abiotic stress responses. Genome. 2018;61(3):151-6.

20. Zhang Y, Tang D, Lin X, Ding M, Tong Z. Genome-wide identification of MADS-box family genes in moso bamboo (Phyllostachys edulis) and a functional analysis of PeMADS5 in flowering. BMC Plant Biol. 2018;18(1):176.

21. Lan P, Li W, Schmidt W. Complementary proteome and transcriptome profiling in phosphate-deficient Arabidopsis roots reveals multiple levels of gene regulation. Mol Cell Proteomics. 2012;11(11):1156-66.

22. Gan CS, Chong PK, Pham TK, Wright PC. Technical, experimental, and biological variations in isobaric tags for relative and absolute quantitation (iTRAQ). J Proteome Res. 2007;6(2):821-7.

23. Wiese S, Reidegeld KA, Meyer HE, Warscheid B. Protein labeling by iTRAQ: a new tool for quantitative mass spectrometry in proteome research. Proteomics. 2007;7(3):340-50.

24. Unwin RD, Griffiths JR, Whetton AD. Simultaneous analysis of relative protein expression levels across multiple samples using iTRAQ isobaric tags with 2D nano LC-MS/MS. Nat Protoc. 2010;5(9):1574-82.

25. Wang X, Zhang X, Zhao L, Guo Z. Morphology and quantitative monitoring of gene expression patterns during floral induction and early flower development in Dendrocalamus latiflorus. Int J Mol Sci. 2014;15(7):12074-93.

26. Hattersley PW. Characterization of C4 type leaf anatomy in grasses (Poaceae). Mesophyll: bundle sheath area ratios. Annals of botany. 1984;53(2):163-80.

27. Minaxi, Saxena J. Disease suppression and crop improvement in moong beans (Vigna radiata) through Pseudomonas and Burkholderia strains isolated from semi arid region of Rajasthan, India. Biocontrol. 2010;55(6):799-810.

28. Marrie TJ, Nelligan J, Costerton JW. A scanning and transmission electron microscopic study of an infected endocardial pacemaker lead. Circulation. 1982;66(6):1339-41.

29. Abràmoff MD, Magalhães PJ, Ram SJ. Image processing with ImageJ. Biophotonics international. 2004;11(7):36-42.

30. Nedbal L, Soukupova J, Kaftan D, Whitmarsh J, Trtilek M. Kinetic imaging of chlorophyll fluorescence using modulated light. Photosynth Res. 2000;66(1-2):3-12.

31. Genty B, Briantais JM, Baker NR. The Relationship between the Quantum Yield of Photosynthetic Electron-Transport and Quenching of Chlorophyll Fluorescence. Biochimica Et Biophysica Acta. 1989;990(1):87-92.

32. Zhang XM, Zhao L, Larson-Rabin Z, Li DZ, Guo ZH. De novo sequencing and characterization of the floral transcriptome of Dendrocalamus latiflorus (Poaceae: Bambusoideae). PloS one. 2012;7(8):e42082.

33. Grabherr MG, Haas BJ, Yassour M, Levin JZ, Thompson DA, Amit I, et al. Full-length transcriptome assembly from RNA-Seq data without a reference genome. Nat Biotechnol. 2011;29(7):644-52.

34. Liu M, Qiao G, Jiang J, Yang H, Xie L, Xie J, et al. Transcriptome sequencing and de novo analysis for Ma bamboo (Dendrocalamus latiflorus Munro) using the Illumina platform. PloS one. 2012;7(10):e46766.

35. Li W, Godzik A. Cd-hit: a fast program for clustering and comparing large sets of protein or nucleotide sequences. Bioinformatics (Oxford, England). 2006;22(13):1658-9.

36. Li B, Dewey CN. RSEM: accurate transcript quantification from RNA-Seq data with or without a reference genome. BMC bioinformatics. 2011;12:323.

37. Robinson MD, McCarthy DJ, Smyth GK. edgeR: a Bioconductor package for differential expression analysis of digital gene expression data. Bioinformatics (Oxford, England). 2010;26(1):139-40.

38. de Hoon MJ, Imoto S, Nolan J, Miyano S. Open source clustering software. Bioinformatics (Oxford, England). 2004;20(9):1453-4.

39. Saldanha AJ. Java Treeview—extensible visualization of microarray data. Bioinformatics (Oxford, England). 2004;20(17):3246-8.

40. Wickham H, Chang W. ggplot2: An implementation of the Grammar of Graphics. R package version 07, URL: http://CRAN R-project org/package= ggplot2. 2008;3.

41. Conesa A, Götz S, García-Gómez JM, Terol J, Talón M, Robles M. Blast2GO: a universal tool for annotation, visualization and analysis in functional genomics research. Bioinformatics. 2005;21(18):3674-6.

42. Tatusov RL, Fedorova ND, Jackson JD, Jacobs AR, Kiryutin B, Koonin EV, et al. The COG database: an updated version includes eukaryotes. BMC Bioinformatics. 2003;4(1):41.

43. Larkin MA, Blackshields G, Brown NP, Chenna R, McGettigan PA, McWilliam H, et al. Clustal W and Clustal X version 2.0. Bioinformatics (Oxford, England). 2007;23(21):2947-8.

44. Tamura K, Peterson D, Peterson N, Stecher G, Nei M, Kumar S. MEGA5: molecular evolutionary genetics analysis using maximum likelihood, evolutionary distance, and maximum parsimony methods. Molecular biology and evolution. 2011;28(10):2731-9.

45. Liu M, Jiang J, Han X, Qiao G, Zhuo R. Validation of reference genes aiming accurate normalization of qRT-PCR data in Dendrocalamus latiflorus Munro. PloS one. 2014;9(2):e87417.

46. Hartigan JA, Wong MA. Algorithm AS 136: A k-means clustering algorithm. Journal of the Royal Statistical Society Series C (Applied Statistics). 1979;28(1):100-8.

47. Fornara F, de Montaigu A, Coupland G. SnapShot: control of flowering in Arabidopsis. Cell. 2010;141(3):550-. e2.

48. Vogel C, Marcotte EM. Insights into the regulation of protein abundance from proteomic and transcriptomic analyses. Nat Rev Genet. 2012;13(4):227-32.

49. Johanson U, West J, Lister C, Michaels S, Amasino R, Dean C. Molecular analysis of FRIGIDA, a major determinant of natural variation in Arabidopsis flowering time. Science. 2000;290(5490):344-7.

50. Liu SN, Zhu LF, Lin XC, Ma LY. Overexpression of the repressor gene PvFRI-L from Phyllostachys violascens delays flowering time in transgenic Arabidopsis thaliana. Biol Plantarum. 2016;60(3):401-9.

51. Michaels SD, Amasino RM. FLOWERING LOCUS C encodes a novel MADS domain protein that acts as a repressor of flowering. The Plant cell. 1999;11(5):949-56.

52. Sakamoto T, Miura K, Itoh H, Tatsumi T, Ueguchi-Tanaka M, Ishiyama K, et al. An overview of gibberellin metabolism enzyme genes and their related mutants in rice. Plant Physiol. 2004;134(4):1642-53.

53. Murase K, Hirano Y, Sun TP, Hakoshima T. Gibberellin-induced DELLA recognition by the gibberellin receptor GID1. Nature. 2008;456(7221):459-63.

54. Ohmori S, Kimizu M, Sugita M, Miyao A, Hirochika H, Uchida E, et al. MOSAIC FLORAL ORGANS1, an AGL6-like MADS box gene, regulates floral organ identity and meristem fate in rice. The Plant cell. 2009;21(10):3008-25.

55. Sung ZR, Belachew A, Shunong B, Bertrand-Garcia R. EMF, an Arabidopsis Gene Required for Vegetative Shoot Development. Science. 1992;258(5088):1645-7.

56. Wu G, Park MY, Conway SR, Wang JW, Weigel D, Poethig RS. The sequential action of miR156 and miR172 regulates developmental timing in Arabidopsis. Cell. 2009;138(4):750-9.

57. Michaels SD, Ditta G, Gustafson-Brown C, Pelaz S, Yanofsky M, Amasino RM. AGL24 acts as a promoter of flowering in Arabidopsis and is positively regulated by vernalization. Plant J. 2003;33(5):867-74.

58. Guo XQ, Wang Y, Wang Q, Xu ZE, Lin XC. Molecular characterization of FLOWERING LOCUS T(FT)genes from bamboo (Phyllostachys violascens). Journal of Plant Biochemistry and Biotechnology. 2016;25(2):168-78.

59. Searle I, Coupland G. Induction of flowering by seasonal changes in photoperiod. EMBO J. 2004;23(6):1217-22.

60. Lin C, Yang H, Guo H, Mockler T, Chen J, Cashmore AR. Enhancement of blue-light sensitivity of Arabidopsis seedlings by a blue light receptor cryptochrome 2. Proc Natl Acad Sci U S A. 1998;95(5):2686-90.

61. Briggs WR, Beck CF, Cashmore AR, Christie JM, Hughes J, Jarillo JA, et al. The phototropin family of photoreceptors. The Plant cell. 2001;13(5):993-7.

62. Ahmad M, Cashmore AR. HY4 gene of A. thaliana encodes a protein with characteristics of a blue-light photoreceptor. Nature. 1993;366(6451):162-6.

63. Fowler S, Lee K, Onouchi H, Samach A, Richardson K, Morris B, et al. GIGANTEA: a circadian clock-controlled gene that regulates photoperiodic flowering in Arabidopsis and encodes a protein with several possible membrane-spanning domains. EMBO J. 1999;18(17):4679-88.

64. Hicks KA, Albertson TM, Wagner DR. EARLY FLOWERING3 encodes a novel protein that regulates circadian clock function and flowering in Arabidopsis. The Plant cell. 2001;13(6):1281-92.

65. Simpson GG, Dean C. Arabidopsis, the Rosetta stone of flowering time? Science. 2002;296(5566):285-9.

66. Hayama R, Coupland G. Shedding light on the circadian clock and the photoperiodic control of flowering. Curr Opin Plant Biol. 2003;6(1):13-9.

67. Somers DE. The physiology and molecular bases of the plant circadian clock. Plant Physiol. 1999;121(1):9-20.

68. Alabadí D, Oyama T, Yanovsky MJ, Harmon FG, Más P, Kay SA. Reciprocal regulation between TOC1 and LHY/CCA1 within the Arabidopsis circadian clock. Science. 2001;293(5531):880-3.

69. Dutta S, Biswas P, Chakraborty S, Mitra D, Pal A, Das M. Identification, characterization and gene expression analyses of important flowering genes related to photoperiodic pathway in bamboo. BMC Genomics. 2018;19(1):190.

70. Hisamoto Y, Kobayashi M. Flowering habit of two bamboo species, Phyllostachys meyeri and Shibataea chinensis, analyzed with flowering gene expression. Plant Species Biology. 2013;28(2):109-17.

71. Kobayashi Y, Weigel D. Move on up, it's time for change--mobile signals controlling photoperiod-dependent flowering. Genes Dev. 2007;21(19):2371-84.

72. Suarez-Lopez P, Wheatley K, Robson F, Onouchi H, Valverde F, Coupland G. CONSTANS mediates between the circadian clock and the control of flowering in Arabidopsis. Nature. 2001;410(6832):1116-20.

73. Samach A, Onouchi H, Gold SE, Ditta GS, Schwarz-Sommer Z, Yanofsky MF, et al. Distinct roles of CONSTANS target genes in reproductive development of Arabidopsis. Science. 2000;288(5471):1613-6.

74. Bernier G, Perilleux C. A physiological overview of the genetics of flowering time control. Plant Biotechnol J. 2005;3(1):3-16.

75. Flexas J, Badger M, Chow WS, Medrano H, Osmond CB. Analysis of the relative increase in photosynthetic O2 uptake when photosynthesis in grapevine leaves is inhibited following low night temperatures and/or water stress. Plant physiology. 1999;121(2):675-84.

76. Mcwilliam JR, Kramer PJ, Musser RL. Temperature-Induced Water-Stress in Chilling-Sensitive Plants. Australian Journal of Plant Physiology. 1982;9(3):343-52.

77. Song S, Qi T, Fan M, Zhang X, Gao H, Huang H, et al. The bHLH subgroup IIId factors negatively regulate jasmonate-mediated plant defense and development. PLoS Genet. 2013;9(7):e1003653.

78. Shan X, Wang J, Chua L, Jiang D, Peng W, Xie D. The role of Arabidopsis Rubisco activase in jasmonate-induced leaf senescence. Plant Physiol. 2011;155(2):751-64.

79. Creelman RA, Mullet JE. Biosynthesis and Action of Jasmonates in Plants. Annu Rev Plant Physiol Plant Mol Biol. 1997;48(1):355-81.

80. Corbesier L, Lejeune P, Bernier G. The role of carbohydrates in the induction of flowering in Arabidopsis thaliana: comparison between the wild type and a starchless mutant. Planta. 1998;206(1):131-7.

81. Griffin TJ, Gygi SP, Ideker T, Rist B, Eng J, Hood L, et al. Complementary profiling of gene expression at the transcriptome and proteome levels in Saccharomyces cerevisiae. Mol Cell Proteomics. 2002;1(4):323-33.

82. Hack CJ. Integrated transcriptome and proteome data: the challenges ahead. Brief Funct Genomic Proteomic. 2004;3(3):212-9.

83. Gallardo K, Firnhaber C, Zuber H, Hericher D, Belghazi M, Henry C, et al. A combined proteome and transcriptome analysis of developing Medicago truncatula seeds: evidence for metabolic specialization of maternal and filial tissues. Mol Cell Proteomics. 2007;6(12):2165-79.

84. Schwanhausser B, Busse D, Li N, Dittmar G, Schuchhardt J, Wolf J, et al. Global quantification of mammalian gene expression control. Nature. 2011;473(7347):337-42.

85. Cooke JE, Weih M. Nitrogen storage and seasonal nitrogen cycling in Populus: bridging molecular physiology and ecophysiology. New Phytol. 2005;167(1):19-30.

86. Wildhagen H, Durr J, Ehlting B, Rennenberg H. Seasonal nitrogen cycling in the bark of ccfield-grown Grey poplar is correlated with meteorological factors and gene expression of bark storage proteins. Tree Physiol. 2010;30(9):1096-110.

87. Kania T, Russenberger D, Peng S, Apel K, Melzer S. FPF1 promotes flowering in Arabidopsis. The Plant cell. 1997;9(8):1327-38.

88. Xu ML, Jiang JF, Ge L, Xu YY, Chen H, Zhao Y, et al. FPF1 transgene leads to altered flowering time and root development in rice. Plant Cell Rep. 2005;24(2):79-85.

Figures

Figure 1 Tissues sampled for RNA-seq and protein analysis of *D. latiflorus*. (A)External morphology of *D. latiflorus* was showed in situ. It is a cluster-growing bamboo. (B)Leaves were selected from the 2rd and 3rd knob of the branch apex. (C)The branches of *D. latiflorus* can be divided into four growth stages during floral transition, including the large vegetable leaves (L0), the small vegetable leaves (L1), large flowering leaves (L2) and small flowering leaves (L3). L0 belong to the vegetable clumps. L1, L2 and L3 belong to the same reproductive ramets with at least one pole blooming.

Figure 2 The statistics of leaf surface, stomata and chlorophyll fluorescence. A.(a) The middle of leaf blades were examined by anatomy (indicated by the red square) (b) Leaf area from L0 to L3 (c) SEM of L0, L1, L2 and L3 (d) Stomatal frequency and stomatal length from L0 to L3 (e) The leaf anatomy (f) The blade thickness, epicuticle thickness and lower epidermis thickness B. The parameters of chlorophyll fluorescence of flowering leaves of *D. latiflorus.* C. The heat map of the measurement parameter from L0 to L3. **$p<0.01$, significant difference; *$p<0.05$, difference by t test

Figure 3 The length distribution of reconstructed reference sequences

Figure 4 Numbers of shared and unique genes. L0 vs L1, L0 vs L2 and L0 vs L3 (A) and Gene ontology classification of L0 vs L1, L0 vs L2 and L0 vs L3 (B).

Figure 5 The different expressed genes from L1 to L3 in the same bamboo clump. A. The venn diagram showing the number of differentially expressed genes between every two

samples and the number of joint differentially expressed genes. B. The clustering of differentially expressed genes. Expression ratios are expressed as Log2. The 8 major clusters obtained by K-means algorithm, repreasenting (a) down-regulated at L2 and up-regulated at L3; (b) up-regulated at L2 and down-regulated at L3; (c) down-regulated from L1 to L3; (d) up-regulated from L1 to L3; (e) up-regulated at L2 and down-regulated at L3, the expression level at L3 is lower than that at L1. C. Hierarchical clustering of the differentially expressed genes.

Figure 6 Senescence-associated genes during floral transition in *D. latiflorus*. A. Heat map showing relative expression of senescence-associated genes in the L0, L1, L2 and L3. Each row represents a gene. Expression differences are shown in different colors. Red means high expression and green means low expression. B. Tabular summary of expression values used to generate the heat map, with high FPKM value combinations highlighted in gray.

Figure 7 The photoperiod pathways depended on the circadian rhythm for unigenes by KEGG annotation. (A) and the actual expression levels CO/FT (B) in different stages of bamboo. (a) CO gene expression level; (b) FT gene expression level. Red square in (A) indicates up-regulation in L3 relative to that in L0, green square indicates down-regulated in L3 relative to that in L3 and bar in (B) denotes standard error. YL0 shows 3 months of bamboo seedings, YL1 shows one year of bamboo seedings, YL2 shows two years of bamboo seedings, YL3 shows five years of bamboo seedings, YL4 shows six years of bamboo seedings. L0, L1, L2 and L3 show the same meaning in the paper.

Figure 8 COG functional classifications of the D. latiflorus proteomics

Figure 9 Different expression proteins in L1 and L2

Figure 10 Concordance between changes in the protein and corresponding transcripts

Figure 11 Summary of some of the biological pathways involved in *D. latiflorus* floral transition

Tables

Table 1 Summary of sequencing data and alignment statistics. 1, 2, 3 represented repeat 1, 2, 3, respectively.

Libray	No. of raw reads	Total length (bp)	Total bases (trimmed)	Total length (bp) of high-quality reads	Mapping ratio % (⩽ 3 bp mismatch)	Mapping ratio % (⩽ 2 bp mismatch)
1-L0	23314262	2331426200	19,915,018	1,737,915,587	91.07	89.18
2-L0	14588714	1415105258	12,092,374	1,060,319,827	80.55	75.77
3-L0	16291476	1580273172	13,306,428	1,144,643,922	81.39	76.68
1-L1	16291392	1629139200	14,184,838	1,220,133,252	93.89	92.7
2-L1	19893454	1929665038	16,461,692	1,415,549,817	82.3	77.71
3-L1	11424758	1108201526	9,568,666	826,388,750	81.64	77.19
1-L2	23885568	2316900096	20,098,070	1,674,574,399	92.71	91.54
2-L2	13408704	1300644288	11,154,754	966,968,998	81.26	76.53
3-L2	16328340	1583848980	13,508,604	1,164,116,872	81.03	76.27
1-L3	20567834	2056783400	18,028,992	1,554,070,513	92.05	90.64
2-L3	16266184	1577819848	13,485,326	1,166,389,856	81.06	76.34
3-L3	14418964	1398639508	11,853,156	1,022,707,425	81.33	76.62

Table 2 Summary for the outcome of reference sequences using four datasets in D. latiflorus

Summary	Number
Total number of unigenes	155,494
Total length	229,730,264
Mean unigene length	1477
N50 (bp)	2069
N90 (bp)	779

Table 3 Statistics of annotation results for *D. latiflorus* unigenes

Sequence file	All	NR	UniprotKB	GO	KEGG
L0_L1-unigene	3179	3045	2552	1861	1289
L0_L2-unigene	1732	1670	1415	988	709
L0_L3-unigene	4376	4129	3430	2478	1719

Table 4 The DEGs of major floral pathway loci and genes between vegetative leaves and flowering leaves (L0 vs L3)

Gene ID	Gene name	Predicted protein	Pathway	Log2FC
Unigene2563	Flowering locus T (FT)	Putative kinase inhibitor	Pathway integrator	-2.81
Unigene123271	SOC1	MADS-box	Pathway integrator	-8.71
Unigene39652	AGL24	MADS-box	Pathway integrator	7.37

Unigene57034	Frigida (Fri)	Coiled-coil domain	Vernalization	-6.04
Unigene49361	Flowering locus C (FLC)	MADS-box	Vernalization	8.37
Unigene110221	VIN3	PHD, VID-domain	Vernalization	6.69
Unigene120387	FCA	RNA-binding	Autonomous	10.74
Unigene132444	FY	Polyadenylation factor	Autonomous	2.64
Unigene132606	GID1	Gibberellin receptor GID1	Gibberellin	8.79
Unigene33012	GA20ox	Gibberellin 20 oxidase 1-B	Gibberellin	-6.88
Unigene29825	SPL9	Squamosa promoter-binding -like protein 9	Age pathway	-6.11
Unigene30392	APETALA1 (AP1)/FRUITFULL (FUL)-like genes MADS14	MADS-box	Meristem identity, Floral organ identity	-8.11
Unigene108692	AGL6	MADS-box	Other flowering gene	10.02
Unigene72731	EMF1	Polycomb-group (Pc-G) proteins	Other flowering gene	7.43

Table 5 The main differential genes of circadian rhythms that regulate flowering during photoperiod between L0 and L3

Gene ID	Gene Annotation	Data base	FPKM		Log2FC
			L0	L3	
Unigene42305	Phytochrome A (Phy A)	NR	0.01	1.09	6.77
Unigene28224	Phytochrome B (Phy B)	NR	0.21	4.23	4.33
Unigene81404	Cryptochrome (Cry)	NR, UNIPROTKB	9.01	54.54	2.60
Unigene10798	Gigantea (GI)	NR, UNIPROTKB	0.42	5.57	3.73
Unigene118524	Two-component response regulator-like APRR5 (PRR5)	UNIPROTKB	0.01	14.92	10.54
Unigene4579	Two-component response regulator-like APRR7 (PRR7)	UNIPROTKB	5.65	0.01	-9.14
Unigene105685	Two-component response regulator-like APRR9 (PRR9)	UNIPROTKB	0.01	9.9	9.95
Unigene91042	Two-component response regulator-like APRR9 (PRR3)	UNIPROTKB	3.98	0.01	-8.64
Unigene105693	Two-component response regulator-like APRR1 (PRR1/TOC1)	UNIPROTKB	83.05	21.21	-1.97
Unigene99793	homeobox-leucine zipper protein HDG6 (FWA)	UNIPROTKB	0.82	4.4	2.42
Unigene2906	protein LHY	UNIPROTKB	0.01	4.02	8.65

Unigene7391	EARLY FLOWERING 3 (ELF3)	NR, UNIPROTKB	0.01	2.13	7.73
Unigene24623	EARLY FLOWERING 4 (ELF4)	NR, UNIPROTKB	0.98	0.01	-6.61
Unigene5825	Protein CCA1	UNIPROTKB	0.69	4.78	2.79
Unigene56852	COP1	UNIPROTKB	13.94	2.17	-2.68
Unigene102233	CRY	NR	4.46	0.82	-2.44
Unigene26943	PIF3	UNIPROTKB	2.41	0.01	-7.91
Unigene26128	SPA1	UNIPROTKB	0.06	2.59	5.43
Unigene75776	PAP1	UNIPROTKB	0.58	15.43	4.73
Unigene148518	CHS	UNIPROTKB	13.97	121.68	3.12
Unigene56158	CK2β	UNIPROTKB	0.24	3.56	3.89
Unigene129590	HY5	UNIPROTKB	1.45	15.35	3.40

Table 6 Pathway enrichment analysis of differential expressed proteins between L1 and L2

Pathway	Different Proteins with	P-value	Pathway ID
Metabolic pathways	248 (43.59%)	0.004136880	ko01100
Ribosome	54 (9.49%)	7.334264e-07	Ko03010
Photosynthesis	29 (5.1%)	8.090652e-06	ko00195
Phenylalanine metabolism	19 (3.34%)	0.01086729	ko00360
Peroxisome	16 (2.81%)	0.004919365	ko04146

Photosynthesis - antenna proteins	15 (2.64%)	1.523186e-06	ko00196
Sulfur metabolism	8 (1.41%)	0.004286712	ko00920
Valine, leucine and isoleucine	8 (1.41%)	0.00915234	ko00290

Table 7 Main different biological pathways of their correlation of transcript-to-protein level changes.

Kyoto Encyclopedia of Genes and Genomes pathway	**Correlation**
Carbon metabolism	1
Photosynthesis	0.913
Starch and sucrose metabolism	0.908
Biosynthesis of secondary metabolites	0.589
Metabolic pathways	0.499
Spliceosome	0.172

Additional Files

Additional file 1: This PDF contains all of the additional material (Figures S1-S7)

Figure S1. The bamboo seedlings of different ages.

Figure S2. Boxplot of the log fragments per kilobase of exon per million fragments mapped (FPKM) expression values.

Figure S3. Boxplot distribution of coefficient of variation, in percentage, among biological replicates.

Figure S4. Quantitative RT-PCR validations.

Figure S5. These unigenes were assigned into different pathways.

Figure S6. Plant hormone signal transduction for unigenes by KEGG annotation.

Figure S7. Phylogenetic analysis of the CONSTANS or CONSTANS-like proteins.

Additional File 2: This excel file contains all of the additional Tables (TablesS1-S5).

Table S1. Primers pairs used for Quantitative Real-Time PCR

Table S2. Expression of the same clump of D. latiflorus flowering biomarkers in floral transition.

Table S3. The pathway and the products involved in the pathway of plant hormone signal transduction.

Table S4. The unigenes that share homology with CONSTANS-like genes.

Table S5. Mobile signals controlling photoperiod-dependent flowering

Additional File 3. Protein Annotation.

Additional File 4. The flowering-related protein in proteomics analysis

Additional File 5. 282 up-regulated in the differentially expressed proteins

Additional File 6. 439 down-regulated in differentially expressed proteins

Additional File 7. The relative change in abundance (L2/L1) is shown as a log2 value from vegetable and flowering leaves in D. latiflorus

Figures

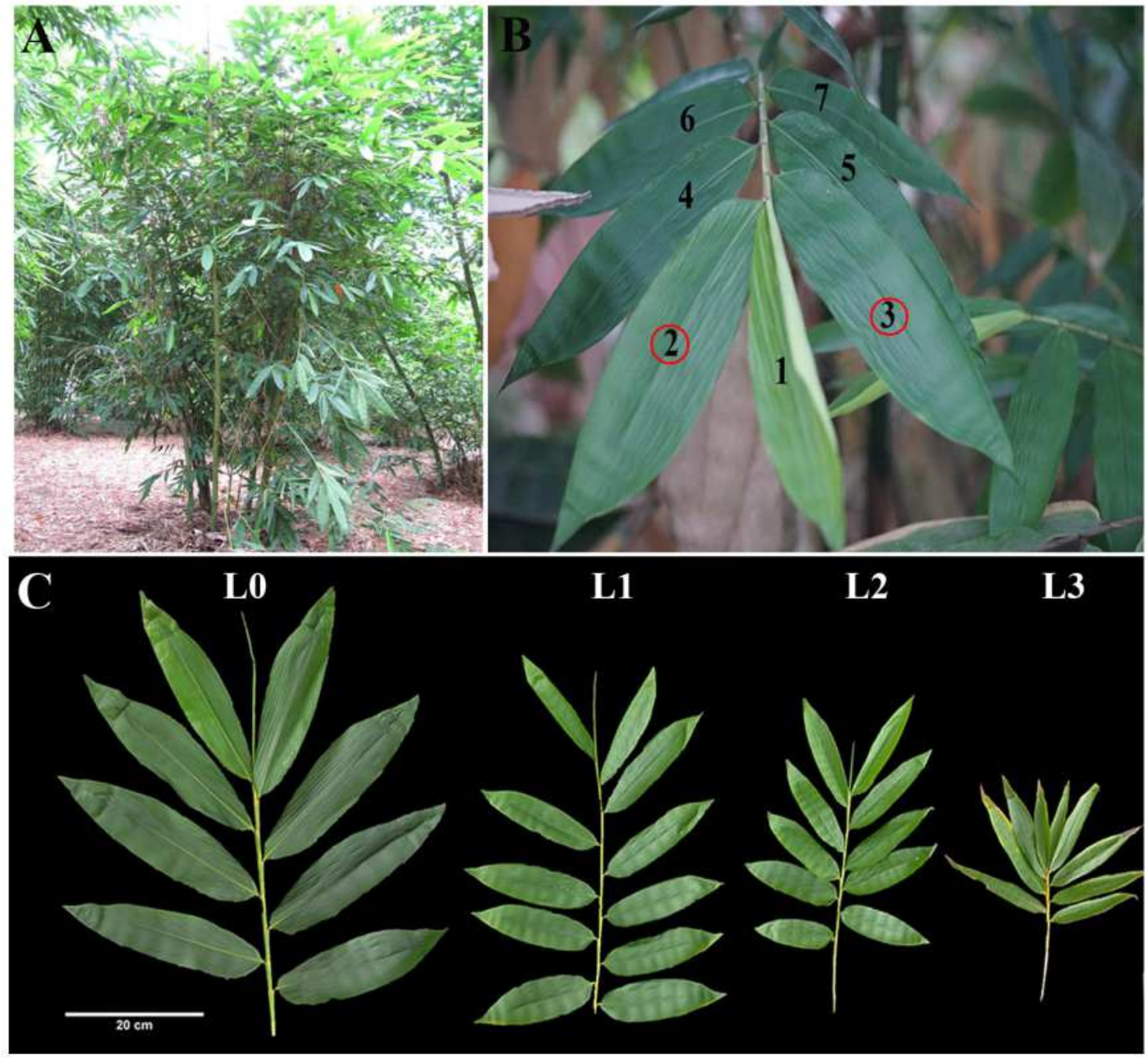

Figure 1

Tissues sampled for RNA-seq and protein analysis of D. latiflorus. (A)External morphology of D. latiflorus was showed in situ. It is a cluster-growing bamboo. (B)Leaves were selected from the 2rd and 3rd knob of the branch apex. (C)The branches of D. latiflorus can be divided into four growth stages during floral transition, including the large vegetable leaves (L0), the small vegetable leaves (L1), large flowering leaves (L2) and small flowering leaves (L3). L0 belong to the vegetable clumps. L1, L2 and L3 belong to the same reproductive ramets with at least one pole blooming.

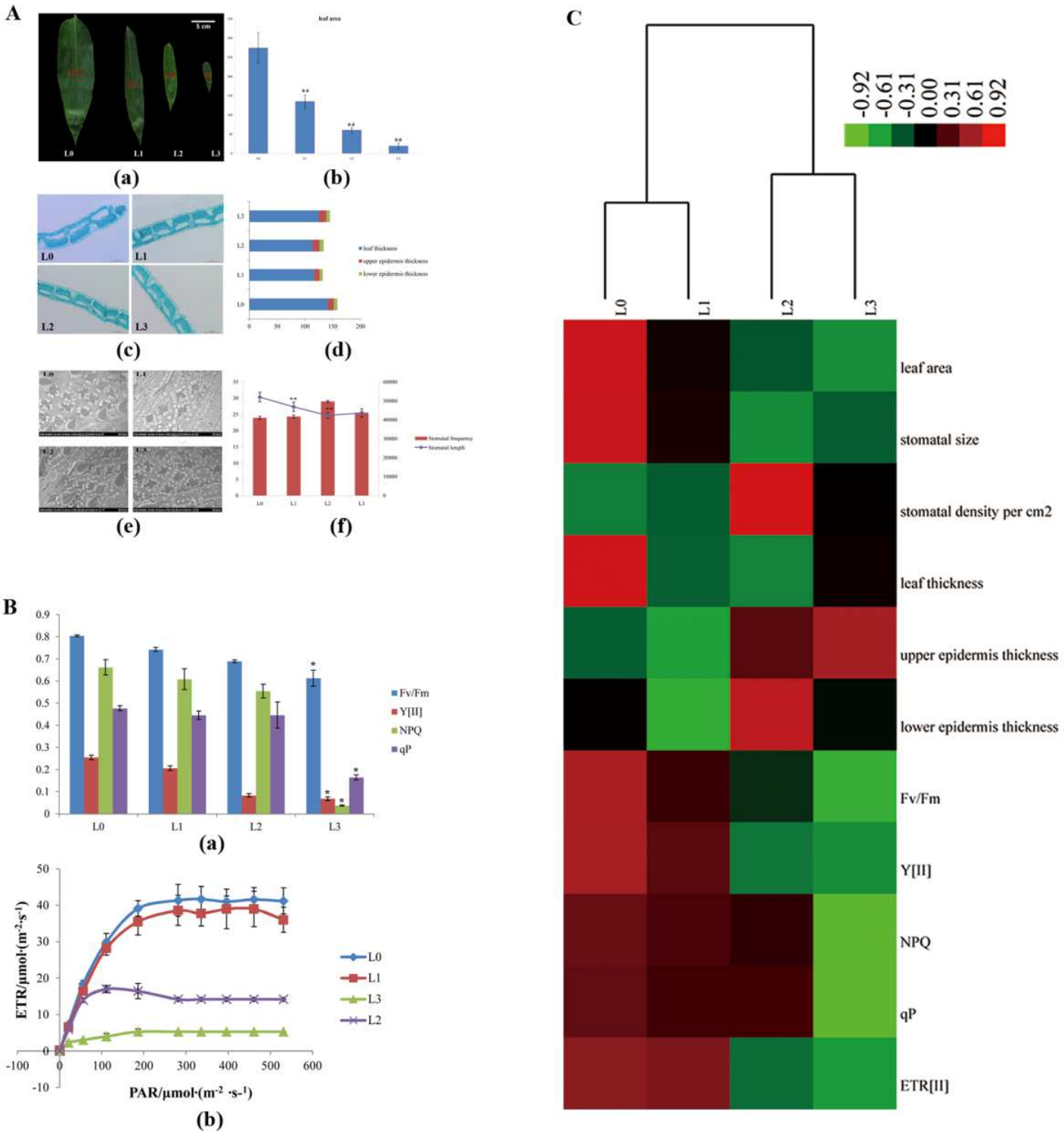

Figure 2

The statistics of leaf surface, stomata and chlorophyll fluorescence. A.(a) The middle of leaf blades were examined by anatomy (indicated by the red square) (b) Leaf area from L0 to L3 (c) SEM of L0, L1, L2 and L3 (d) Stomatal frequency and stomatal length from L0 to L3 (e) The leaf anatomy (f) The blade thickness, epicuticle thickness and lower epidermis thickness B. The parameters of chlorophyll

fluorescence of flowering leaves of D. latiflorus. C. The heat map of the measurement parameter from L0 to L3. **p<0.01, significant difference; *p<0.05, difference by t test

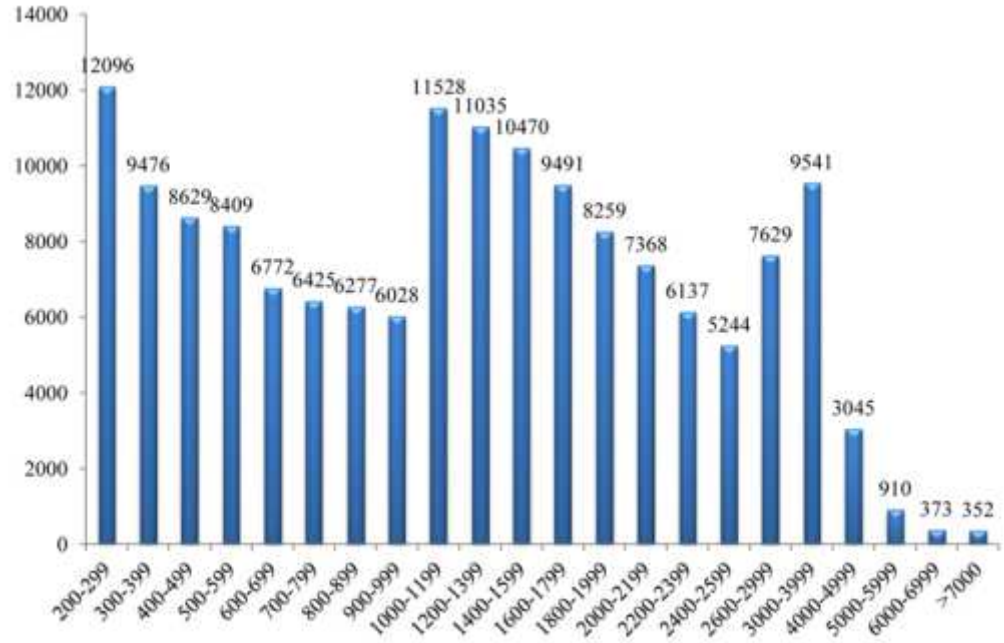

Figure 3

The length distribution of reconstructed reference sequences

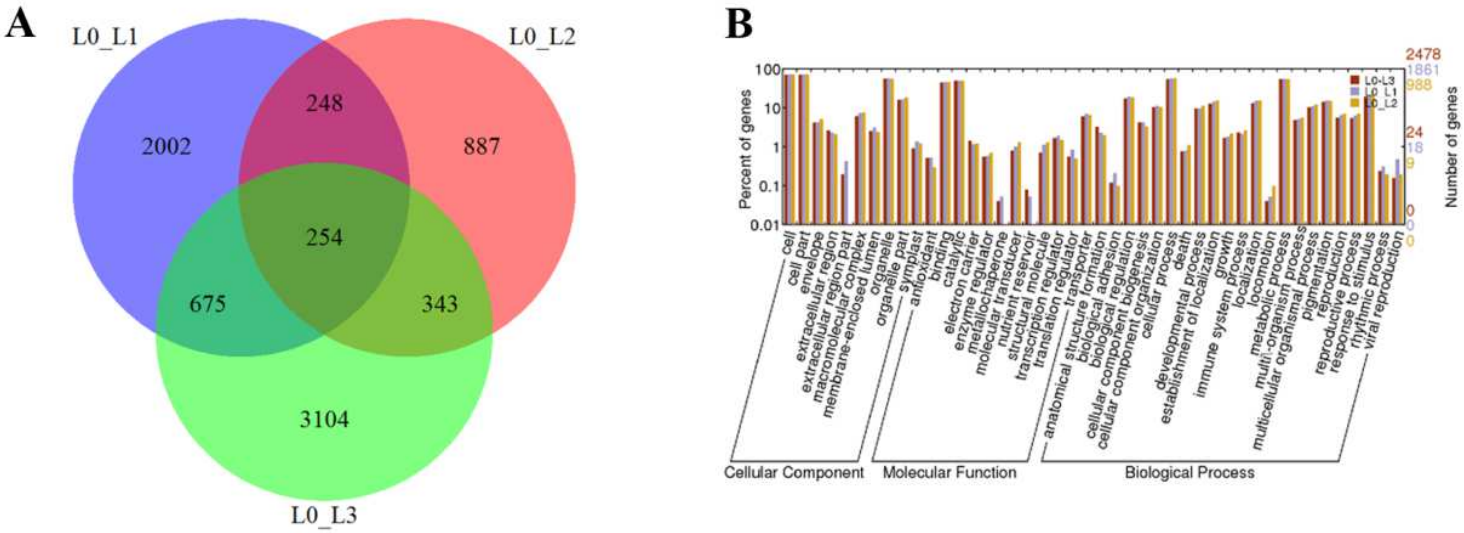

Figure 4

Numbers of shared and unique genes. L0 vs L1, L0 vs L2 and L0 vs L3 (A) and Gene ontology classification of L0 vs L1, L0 vs L2 and L0 vs L3 (B).

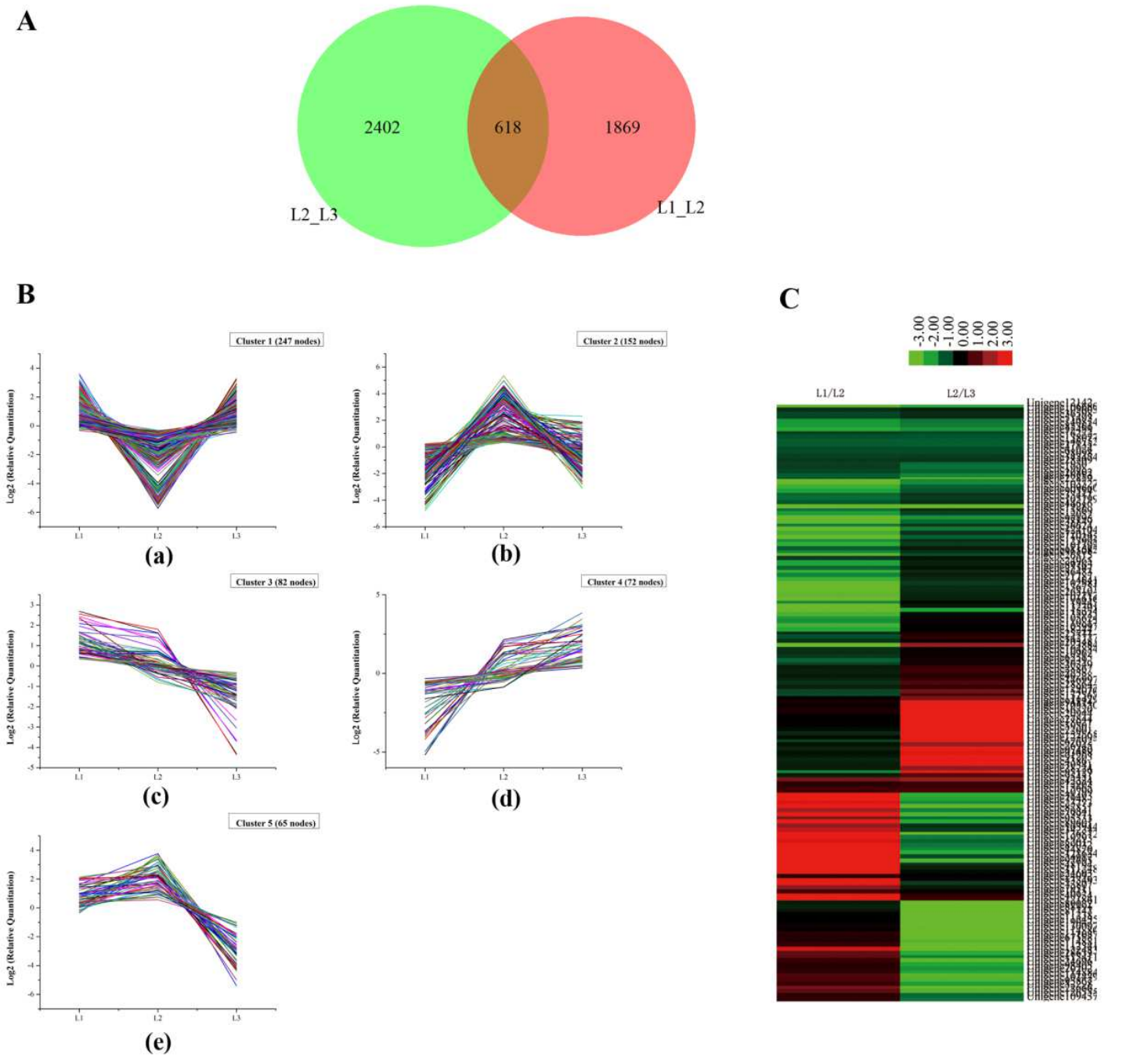

Figure 5

The different expressed genes from L1 to L3 in the same bamboo clump. A. The venn diagram showing the number of differentially expressed genes between every two samples and the number of joint differentially expressed genes. B. The clustering of differentially expressed genes. Expression ratios are expressed as Log2. The 8 major clusters obtained by K-means algorithm, repreasenting (a) down-regulated at L2 and up-regulated at L3; (b) up-regulated at L2 and down-regulated at L3; (c) down-regulated from L1 to L3; (d) up-regulated from L1 to L3; (e) up-regulated at L2 and down-regulated at L3, the expression level at L3 is lower than that at L1. C. Hierarchical clustering of the differentially expressed genes.

A

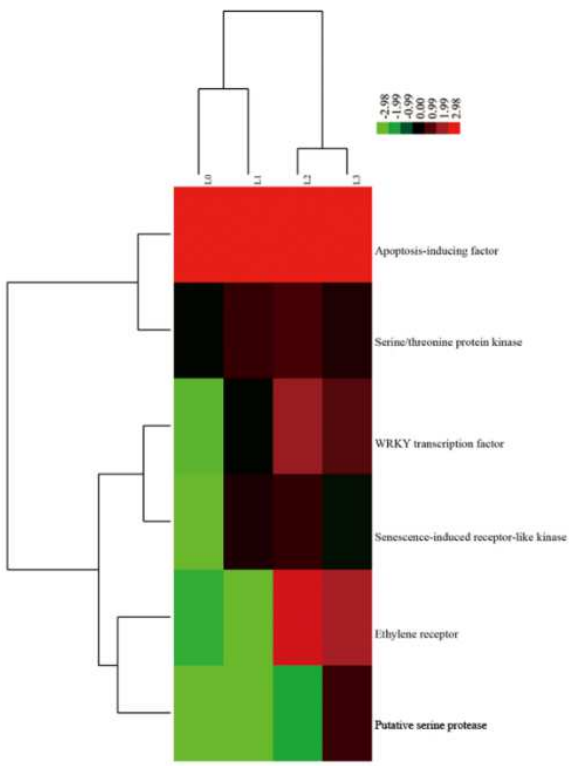

B

Gene ID	Functional description	Accession	E-value	FPKM			
				L0	L1	L2	L3
Unigene108536	Putative serine protease	sp|P90893	6e-29	0.01	0.04	0.24	1.62
Unigene118824	Serine/threonine protein kinase	sp|P13185	1e-40	0.92	1.59	1.8	1.31
Unigene25575	Apoptosis-inducing factor	sp|Q96NN9	5e-26	30.27	40.86	52.33	148.67
Unigene26011	WRKY transcription factor	sp|Q9SZ67	1e-06	0.15	0.93	3.69	2.06
Unigene28224	Ethylene receptor	sp|Q9ZWL6	2e-20	0.21	0.01	6.13	4.23
Unigene28507	Senescence-induced receptor-like kinase	sp|O64483	7e-43	0.01	1.28	1.53	0.88

Figure 6

Senescence-associated genes during floral transition in D. latiflorus. A. Heat map showing relative expression of senescence-associated genes in the L0, L1, L2 and L3. Each row represents a gene. Expression differences are shown in different colors. Red means high expression and green means low expression. B. Tabular summary of expression values used to generate the heat map, with high FPKM value combinations highlighted in gray.

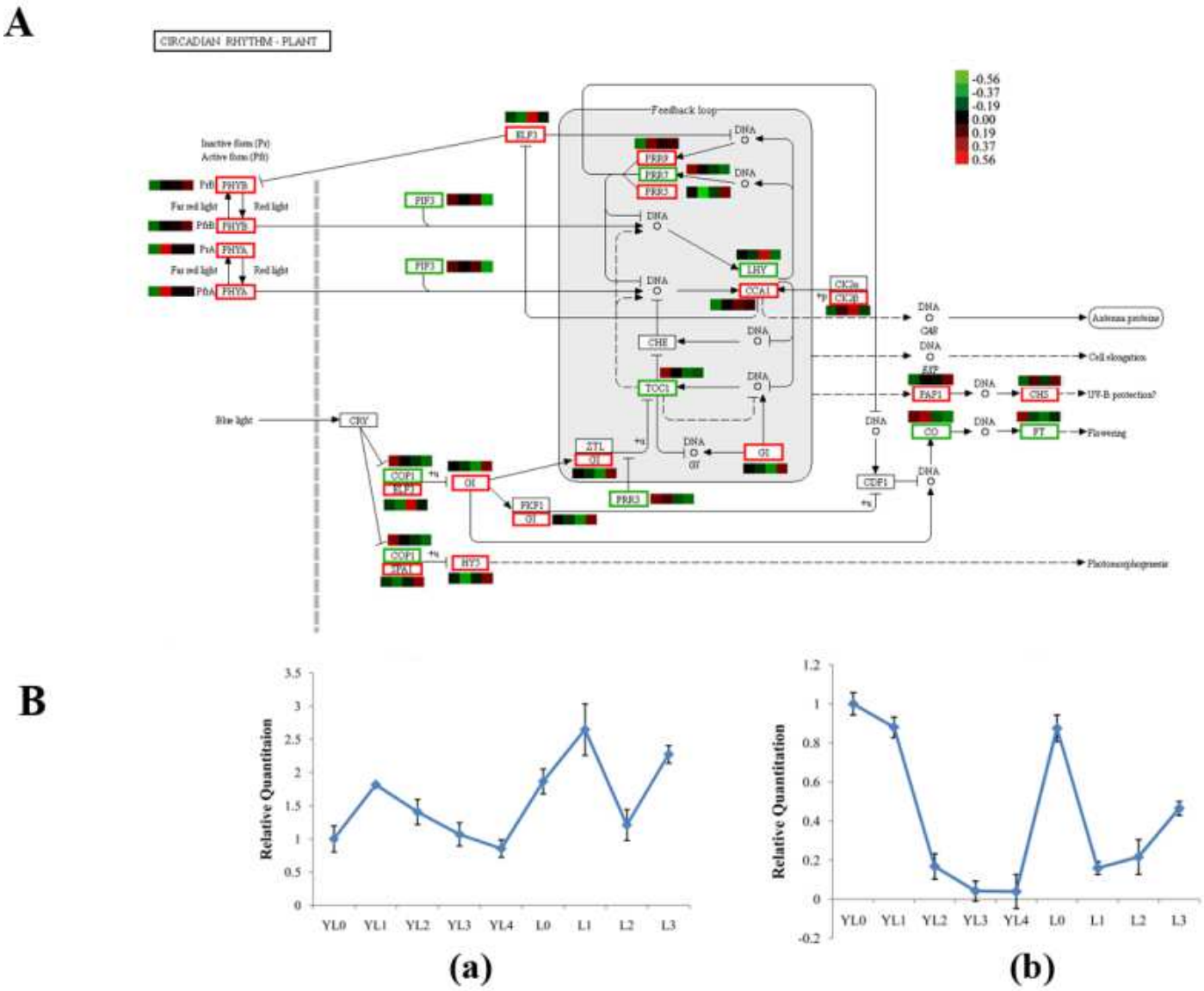

Figure 7

The photoperiod pathways depended on the circadian rhythm for unigenes by KEGG annotation. (A) and the actual expression levels CO/FT (B) in different stages of bamboo. (a) CO gene expression level; (b) FT gene expression level. Red square in (A) indicates up-regulation in L3 relative to that in L0, green square indicates down-regulated in L3 relative to that in L3 and bar in (B) denotes standard error. YL0 shows 3 months of bamboo seedings, YL1 shows one year of bamboo seedings, YL2 shows two years of bamboo seedings, YL3 shows five years of bamboo seedings, YL4 shows six years of bamboo seedings. L0, L1, L2 and L3 show the same meaning in the paper.

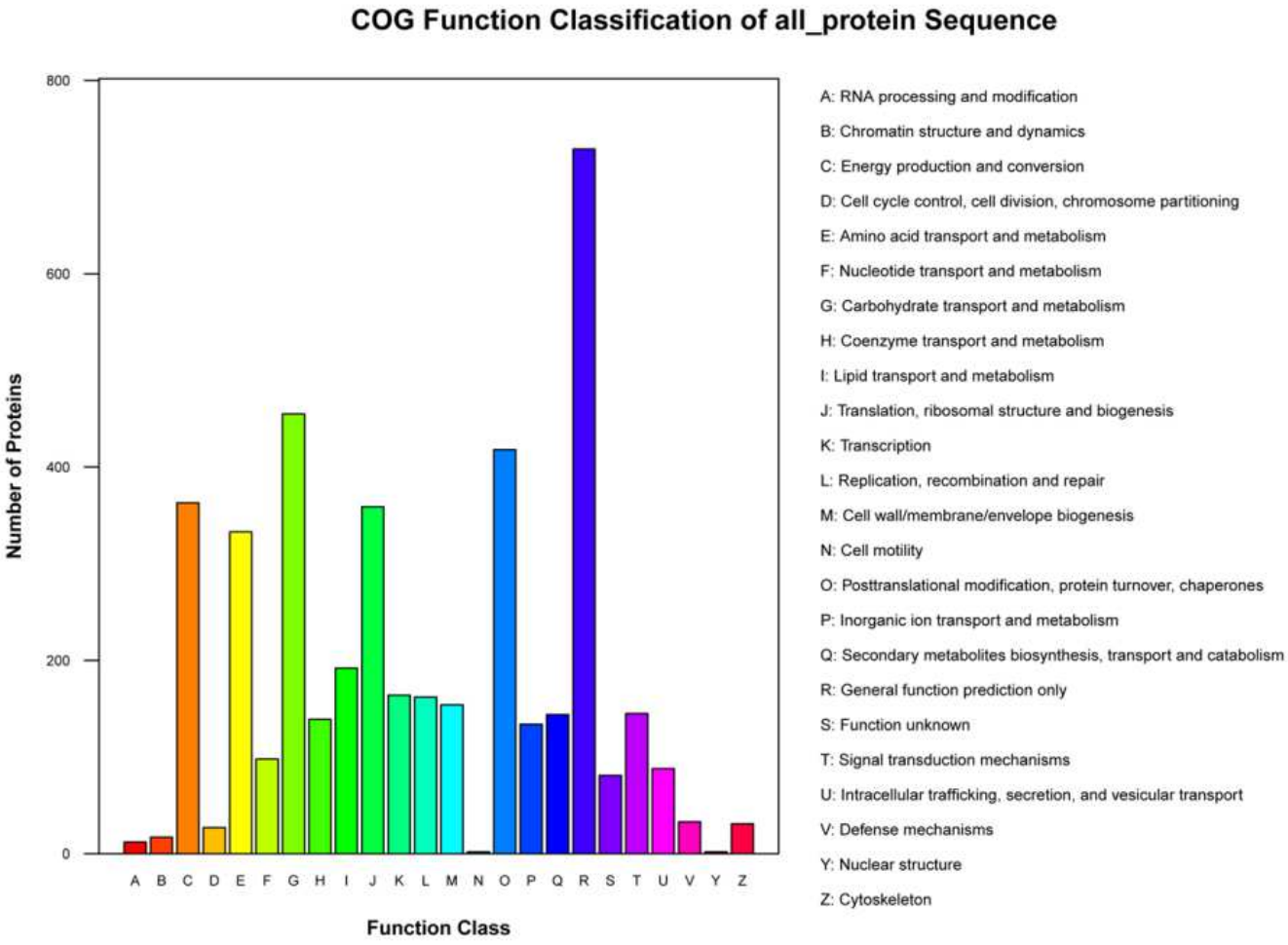

Figure 8

COG functional classifications of the D. latiflorus proteomics

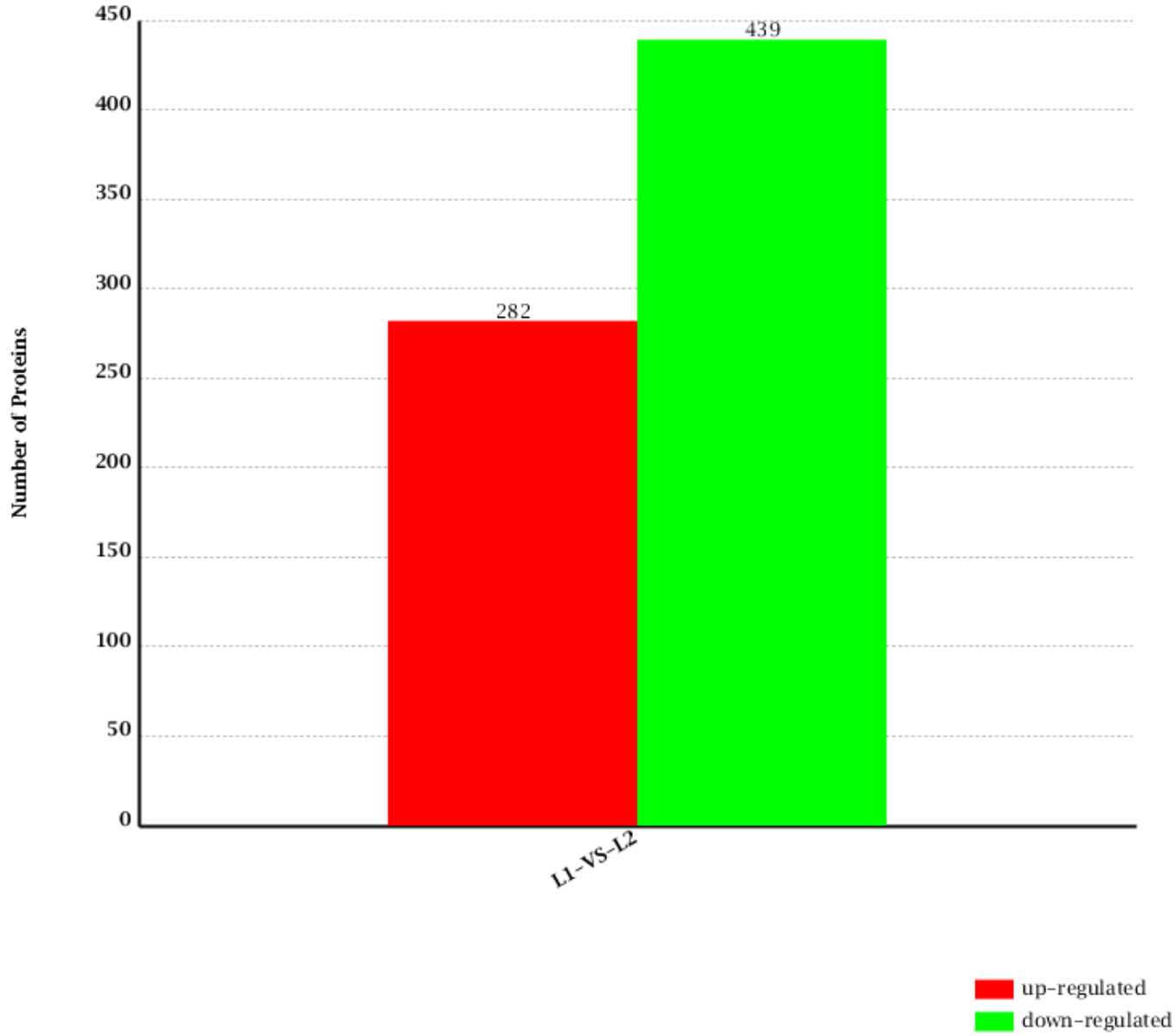

Figure 9

Different expression proteins in L1 and L2

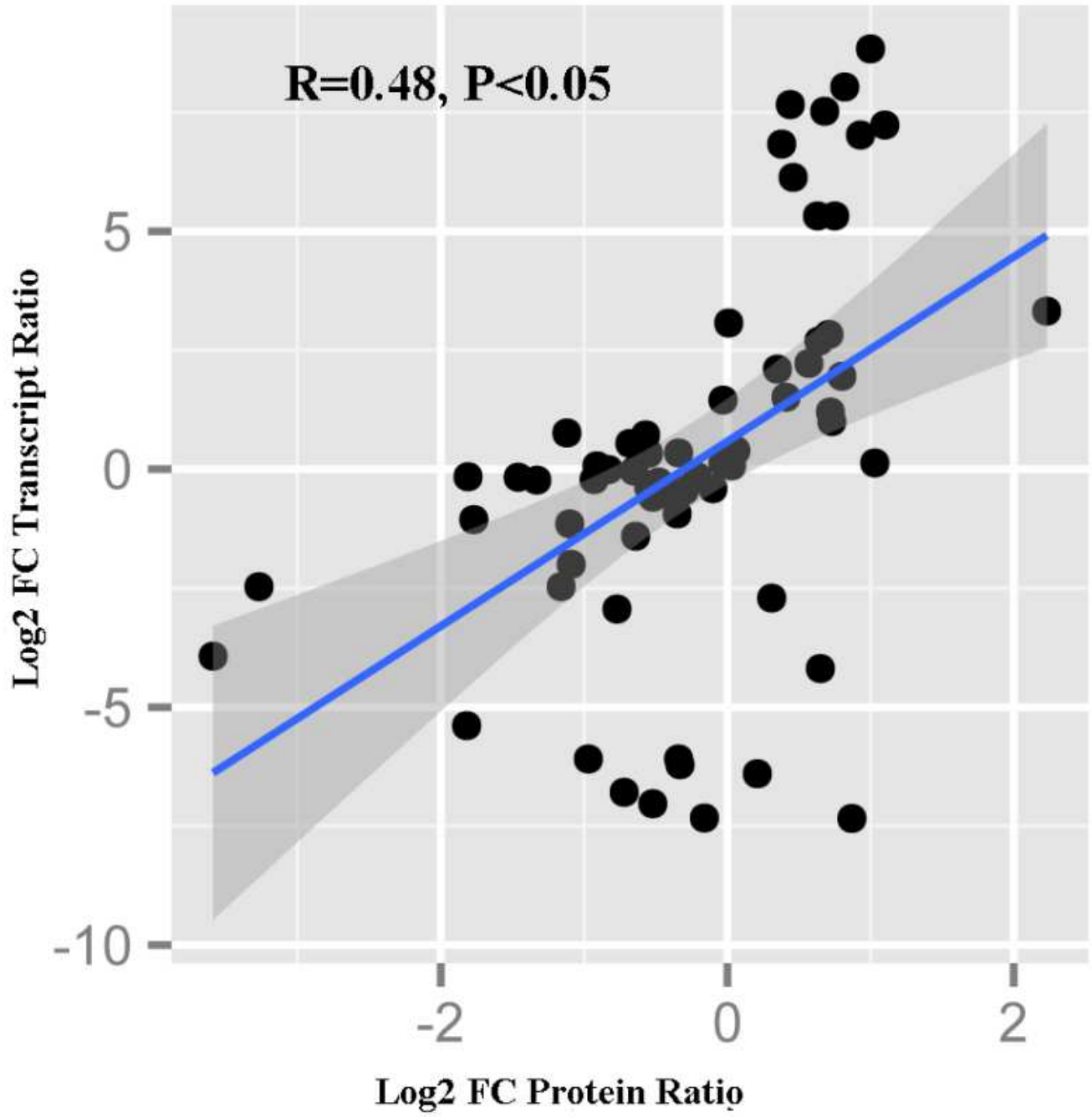

Figure 10

Concordance between changes in the protein and corresponding transcripts

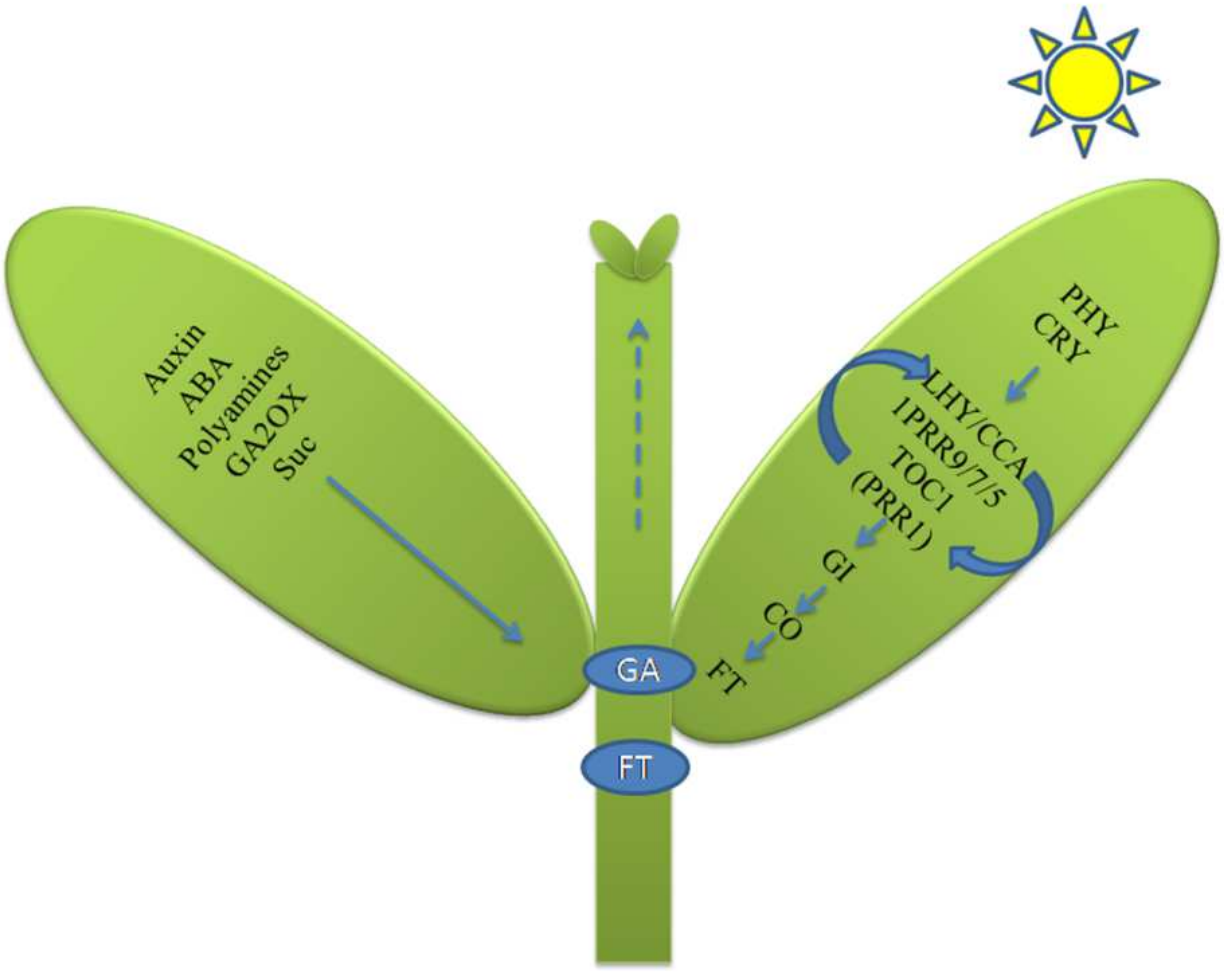

Figure 11

Summary of some of the biological pathways involved in D. latiflorus floral transition

Supplementary Files

This is a list of supplementary files associated with this preprint. Click to download.

- Additionalfile6.xlsx
- Additionalfile5.xlsx
- Additionalfile7.xlsx
- Additionalfile2.pdf
- Additionalfile4.xlsx
- Additionalfile3.xlsx
- Additionalfile1.pdf